IMPROVED MODEL FOR REINFORCED CONCRETE MEMBERS SUBJECTED TO COMBINED LOADING INCLUDING TORSION

SMRITHI P HAREENDRAN

CE14MTECH11007

A Dissertation Submitted to

Indian Institute of Technology Hyderabad

In Partial Fulfilment of the Requirements for

The Degree of Master of Technology

DEPARTMENT OF CIVIL ENGINEERING

INDIAN INSTITUTE OF TECHNOLOGY HYDERABAD

JUNE, 2016.

Declaration

I declare that this written submission represents my ideas in my own words, and where others' ideas or words have been included, I have adequately cited and referenced the original sources. I also declare that I have adhered to all principles of academic honesty and integrity and have not misrepresented or fabricated or falsified any idea/data/fact/source in my submission. I understand that any violation of the above will be a cause for disciplinary action by the Institute and can also evoke penal action from the sources that have thus not been properly cited, or from whom proper permission has not been taken when needed.

Smrithi P Hareendran
ce14mtech11007

Approval Sheet

This thesis entitled **"Improved Model for Reinforced Concrete Members under Combined Loading Including Torsion"** by Smrithi P Hareendran is approved for the degree of Master of Technology from IIT Hyderabad.

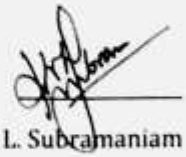

Prof. K. V. L. Subramaniam

Examiner

Dr. Anil Agarwal

Examiner

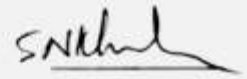

Dr. Syed Nizamuddin Khaderi

Examiner

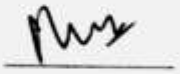

Dr. S. Suriya Prakash

Advisor

ABSTRACT

Majority of the concrete structural components in general are subjected to different load combinations. The internal forces acting on any section in general can be categorized into four basic actions. These are (a) Flexural moments, (b) Axial loads, (c) Shear forces and (d) Torsion. These actions may occur alone or in combination with others and they effect the structures in different ways under various conditions. Some of these combinations can include significant shear and torsion. The shear and bending forces acting maybe lateral (along Z- axis) or vertical (along Y-axis). The action of all the sectional forces are shown in Fig.1.1. The behaviour of RC members under combinations of flexure, shear and axial load has been relatively well understood. Whereas, the behavior under shear and torsion are more complicated and the detailed studies conducted on these are very limited. There are several studies conducted to study the behavior under torsion and the earlier models developed could predict only the ultimate loads carried by the section. The latest model available is the Combined Action Softened Truss Model (CASTM), developed by Dr. Gary Greene Jr. in the year 2006. This research is aimed to study the existing CASTM and to improve upon the model using the latest stress-strain relationships for material components and also to incorporate the improved constitutive relationships for strains.

CONTENTS

DECLARATION ERROR! BOOKMARK NOT DEFINED.

DECLARATION *ERROR! BOOKMARK NOT DEFINED.*

APPROVAL SHEET ERROR! BOOKMARK NOT DEFINED.

APPROVAL SHEET *ERROR! BOOKMARK NOT DEFINED.*

ABSTRACT *4*

LIST OF FIGURES *7*

LIST OF TABLES *9*

CHAPTER - 1 *11*

INTRODUCTION *11*

1.1. TORSION *12*

1.2. RESEARCH SIGNIFICANCE *13*

1.3. OBJECTIVES AND SCOPE *14*

1.4. OVERVIEW OF THE THESIS *14*

CHAPTER - 2 *17*

LITERATURE REVIEW *17*

2.1. BACKGROUND TO BEHAVIOR UNDER TORSION *17*

2.1.1. BEHAVIOUR OF CONCRETE IN PRE-CRACKING STAGE 17

2.1.2. BEHAVIOR OF CONCRETE POST - CRACKING: 18

2.2. SKEW BENDING THEORY: *18*

2.3. DIAGONAL COMPRESSION FIELD THEORY (CFT): *20*

2.4. SOFTENED TRUSS MODEL (STM) *22*

2.5. MODIFIED COMPRESSION FIELD THEORY (MCFT) *23*

2.6. TENSION STIFFENED SOFTENED TRUSS MODEL (TS-STM) *24*

CHAPTER-3 *26*

COMBINED ACTION SOFTENED TRUSS MODEL *26*

3.1. INTRODUCTION *26*

3.2. BASIC ASSUMPTIONS OF THE MODEL *26*

3.3. MODEL CROSS SECTION *28*

3.4. BACKGROUND FOR THE DEVELOPMENT OF CA-STM *28*

3.5. BIAXIAL STRESS-STRAIN RELATIONSHIPS FOR CONCRETE *30*

3.5.1. Compression softening 30
3.5.2. Tension Stiffening 32

3.6. STRESS-STRAIN RELATIONSHIPS OF REINFORCEMENT *35*

3.7. BREDT'S THIN TUBE THEORY *36*

3.8. DISTRIBUTION OF APPLIED LOADS *37*

3.9. EQUILIBRIUM AND STRAIN COMPATIBILITY *39*

3.10. STRESS-STRAIN DISTRIBUTION IN CONCRETE *41*

3.10.1. Strain Distribution: 41
3.10.2. Stress Distribution: 42

3.11. STRAIN COMPATIBILITY AMONG PANELS *43*

3.11.1. Longitudinal and Transverse curvature in panels: 43
3.11.2. Longitudinal strain compatibility among panels: 44
3.11.3. Twist on concrete strut: 45
3.11.4. Curvature of concrete strut: 45

*3.12. SHEAR FLOW ZONE INDEX (*ZI*)* *46*

3.13. DISTRIBUTION OF LONGITUDINAL REINFORCEMENT *48*

3.14. ADDITIONAL EQUATIONS *51*

3.15. METHOD OF SOLUTION OF CA-STM *52*

3.15.1. SOLUTION PROCEDURE 53

CHAPTER-4 *58*

VALIDATION OF RESULTS AND DISCUSSION *58*

4.1. INTRODUCTION: *58*

4.2. RESPONSE OF MEMBERS UNDER PURE TORSION *59*

4.2.1. McMullan and Warwaruk Specimens: 59
4.2.2. Lampert and Thurliman Specimens: 60

4.3. TORSION COMBINED WITH SHEAR (RAHAL AND COLLINS) *62*

4.4. TORSION COMBINED WITH AXIAL FORCE AND BENDING MOMENT *66*

CHAPTER 5 *70*

SUMMARY AND CONCLUSIONS *70*

5.1. CONCLUSIONS *70*

5.2. SCOPE FOR FURTHER WORK: *71*

5.3 REFERENCES: *72*

LIST OF FIGURES

Fig. No	Name of the figure	Pg.No
1.1	Member subjected to combined section forces	11
1.2	Torsion acting in outrigger beams	12
1.3	Types of cross sections for a bridge girder	14
2.1	Crack propagation in concrete sections under torsion	18
2.2	Modes of failure assumed in Skew Bending Theory	19
2.3	Cross section of a shear panel	21
2.4(a)	Strain distribution across the shear flow zone	22
2.4(b)	Compression softening of concrete	22
3.1	Model cross section details	28
3.2	Softened stress-strain relationship for concrete in compression	31
3.3	Average stress-strain response of concrete in tension	32
3.4	sectional details for calculation of cracking stress of concrete	34
3.5	Normalized stress-strain variation of concrete in tension	35
3.6	Representation of a thin tube under torsion	36
3.7	Generic forces acting on an RC section	37
3.8	Distribution of shear force and Torsion in each panel	38
3.9	Distribution of bending moments and Normal forces in panels	39
3.10	RC membrane element with the co-ordinate axes	40
3.11	Stress-strain distribution in concrete over the shear flow zone	41
3.12	Longitudinal and transverse curvatures in panels	43
3.13	Longitudinal strain compatibility	44
3.14	Curvature in concrete strut	46
3.15	Shear flow zone index	47
3.16	Idealization of RC section for distribution of longitudinal reinforcement	49
3.17	Equal force assumption for distribution of longitudinal reinforcement	50
4.1	Cross sectional details of McMullen and Warwaruk specimens	59

4.2	Validation of improved CASTM with experimental data under torsion	60
4.3	Cross sections of Lampert and Thurliman specimens	61
4.4	Validation of CASTM model for pure torsion	62
4.5	Experimental setup for Rahal and Collins specimens	63
4.6	Cross sectional details of the specimen	63
4.7	Comparison of results for series 1	64
4.8	Comparison of results for series 2	65
4.9	Cross section of Tirasit column	66
4.10	Behavior of RC column under combined torsion and bending	67

LIST OF TABLES

Table. No	Name of the table listed	Pg. No
4.1	Cross sectional details of McMullen and Warwaruk specimen	59
4.2	Cross sectional details of Lampert and Thurliman specimens	61
4.3	Specimen details of Rahal and Collins experimental study	62
4.4	Details of RC columns of Tirasit specimen	66
4.5	Comparison of results obtained with experimental data	68

CHAPTER – 1

INTRODUCTION

CHAPTER - 1

INTRODUCTION

Majority of the concrete structural components in general are subjected to different load combinations. The internal forces acting on any section in general can be categorized into four basic actions. These are (a) Flexural moments, (b) Axial loads, (c) Shear forces and (d) Torsion. These actions may occur alone or in combination with others and they effect the structures in different ways under various conditions. Some of these combinations can include significant shear and torsion. The shear and bending forces acting maybe lateral (along Z- axis) or vertical (along Y-axis). The action of all the sectional forces are shown in Fig.1.1. The behaviour of RC members under combinations of flexure, shear and axial load has been relatively well understood. Whereas, the behavior under shear and torsion are more complicated and the detailed studies conducted on these are very limited.

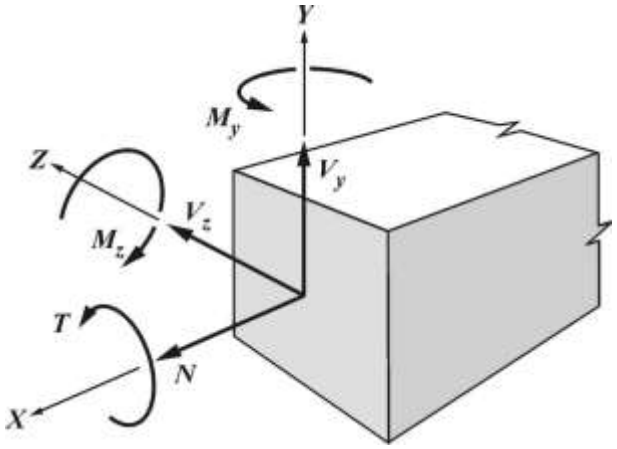

Figure 1.1 Member subjected to combined section forces [Reference. 1]

1.1. TORSION

Torsion can be a significant action in many of the structural members. Torsion is exhibited in: (a) Curved bridges (b) Elevated guide ways and (c) Spandrel beams under gravity loads. During the occurrence of a seismic event, the column connectors, beams and columns of bridges with outriggers are subjected to cyclic torsion. This can also act in combination with other actions such as bending and shear. These conditions necessitates the study of effects of torsion and combination of torsion with other actions on various structural members. Reliable models should also be generated which can predict the member's capacity and load-deformation response under these actions.

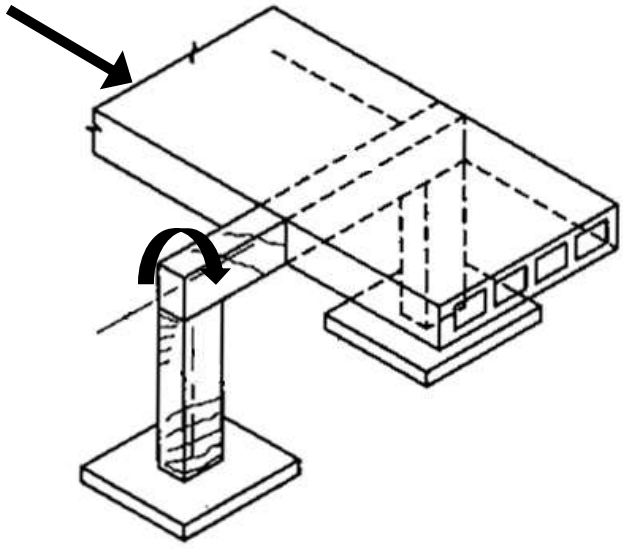

Figure 1.2 Torsion acting on outrigger bents [Reference. 2]

1.2. RESEARCH SIGNIFICANCE

The study of torsional response of reinforced concrete structures became significant only in the 1960s, when computer analysis made it practical to calculate the torsional moments. There are several studies conducted to study the behavior under torsion and the earlier models developed could predict only the ultimate loads carried by the section. Such models to predict the capacity under torsional loads were based on skew bending approach. Although these models could predict the torsional capacity at failure, they were deficient because they were only developed considering equilibrium conditions and therefore could not predict the member's deformation. Later, truss models were developed that could predict the envelope of the load-deformation response for members under pure torsion (Mitchell and Collins 1974; Hsu and Mo 1985a) or combined actions including torsion (Rahal and Collins, 1995; Greene and Belarbi 2006).

The latest model available is the Combined Action Softened Truss Model (CASTM), developed by Dr. Gary Greene Jr. in the year 2006. This research is aimed to study the existing CASTM and to improve upon the model using the latest stress-strain relationships for material components and also to incorporate the improved constitutive relationships for strains.

The model is initially developed for a rectangular box section. The section was chosen primarily because they are commonly used in bridge decks. Box sections are preferred for its high torsional stiffness Moreover, horizontally curved bridges, the box

girders also have high ratio of strength to weight and also high ratio of stiffness to weight.

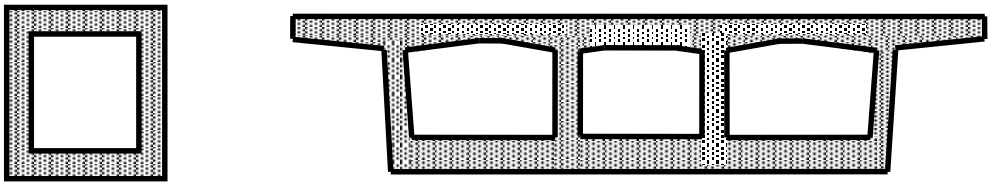

a)singe cell box section b)multiple cell box section

Figure 1.3 Types of Cross Sections for Bridge Girder [Reference. 1]

1.3. OBJECTIVES AND SCOPE

The main objective of the study was to improve the existing Combined Action Softened Truss Model using latest available constituive models and predict the behavior of reinforced concrete members. The developed analytical model should be capable of predicting the behavior under any combination of loads including Torsion, Shear, Bending and Axial loads. The scope of this work includes (i) To develop combined action softened truss model using Matlab, (2) to validate the developed model using test data of different experimental studies conducted on reinforced concrete members under various loading conditions for both beams and columns.

1.4. OVERVIEW OF THE THESIS

In chapter 2 of the thesis, the background to the development of CA-STM is given. The behavior of concrete under torsion is explained in the first section. Then the various models developed prior to CA-STM for the prediction of behavior of RC

members under different loading conditions is introduced. The limitations of each of the models are also explained. Chapter 3 explains the development of mathematical formulations in the model. It also explains the procedure and the algorithm followed in the development of the model. Chapter 4 explains the validations done for the developed model. It also explains the details of experimental studies conducted on the specimens referred to. The conclusions are mentioned in chapter 5.

CHAPTER-2

LITERATURE REVIEW

CHAPTER - 2

LITERATURE REVIEW

2.1. BACKGROUND TO BEHAVIOR UNDER TORSION

2.1.1. Behaviour of concrete in Pre-cracking stage

Torsion induces shear stresses and causes warping of non-circular sections. The principal tensile and compressive stress trajectories spiral around the beam in orthogonal directions at 45° to the beam axis. One such line is shown in Fig 2.1. The principal tensile stress acts across the crack shown in Figure. Such a crack would develop in a concrete beam when the diagonal tensile stress reaches the tensile strength of concrete. Owing to the brittle nature of concrete such a crack would rapidly propagate inwards from the outer surface. This effectively destroys the torsional resistance of the member which is primarily contributed by the fibers in the outermost layers. This is the point corresponding to the ultimate torsional resistance of a plain concrete section. The same is considered to be the cracking torque for a reinforced concrete section. Thus before cracking, an RC member behaves as if it were a homogeneous member and behaves elastically, and the shear stresses induced by the applied torque are resisted by the concrete alone. There are many theories developed to predict the cracking torque and twist (Hsu, 1968).

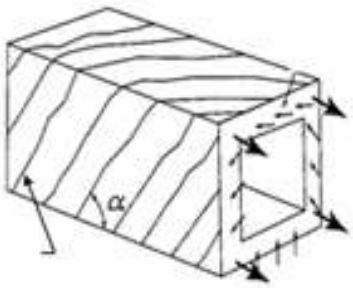

Figure 2.1 Crack propagation of concrete sections subjected to torsion [Reference. 3]

2.1.2. Behavior of concrete Post - Cracking:

The behavior of an RC member under torsion is significantly different before and after cracking. There are many theories to predict the effect of various loadings on RC members after cracking. These include Skew bending theory, diagonal compression field theory and Softened truss models. Each of the theories and their limitations are discussed in the following sub sections. Torsion induces diagonal cracking along the member. After diagonal cracks are formed, it divides the member into a series of concrete struts. The shear from the applied torque is thereafter resisted by a truss, with the concrete in compression and the reinforcement in tension. Twisting in a non-circular member under torsion will also cause the initially plane surfaces to warp. The warping induces a bending moment in the concrete struts in addition to the compressive forces. These concepts form the basis for the theories explained below.

2.2. SKEW BENDING THEORY:

Skew bending theories are used to predict the ultimate loads carried by the member. The theory uses equilibrium equations to calculate the loads acting at failure. The theory assumes that the cracks are formed in a helical pattern around the surface of

the member and create a skew failure surface with the compression zone inclined at an angle to the beam's longitudinal axis. This creates a skewed surface of failure with the compression zone inclined at an angle to the longitudinal axis of the beam. The model assumes a failure mode from the two failure modes, Mode I and Mode II as shown below.

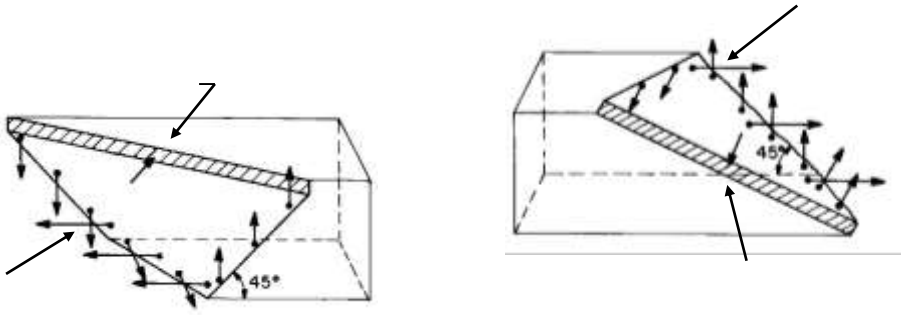

Figure 2.2 Two modes of failure assumed in Skew Bending Theory [Reference. 2]

Internal torsional and bending resistance was calculated by assuming a failure mode from the two mentioned above and then equilibrium equations were derived by summing moments about the failure surface. After cracking, the applied torque is resisted by a field of compressive stresses spiraling around the beam following the crack pattern. The resulting compressive forces inclined to the longitudinal axis induces tensile stresses in the longitudinal and transverse reinforcement.

The crack angle along a face of the member was either assumed to be 45° or was calculated based on the relative force that could be developed in the longitudinal and transverse reinforcement assuming yield stresses in both. The diagonally inclined

compressive stresses provides the shear flow around the section that equilibrates the applied torque. The major limitations of the skew bending theory are:

- It neglects the compression softening of concrete under biaxial stresses, tensile strength of concrete and also the dowel action in the reinforcement.
- The warping in the cross section due to torsion is also neglected.
- The theory considers only equilibrium of forces. Hence it cannot predict the deformation response of the member.
- The theory assumes that the transverse and longitudinal reinforcement has yielded and hence this theory cannot be applied to over reinforced sections.

2.3. DIAGONAL COMPRESSION FIELD THEORY (CFT):

CFT is the first theory to satisfy the equilibrium, strain compatibility and material laws. It was developed by Mitchell and Collins in 1974. The model idealizes the member's cross section into a shear panel with the thickness equal to shear flow zone (based on Bredt's thin tube theory to be explained later in next section). The equilibrium and compatibility are formulated for the shear panel.

Compression field theory uses uniaxial stress-strain relationship for concrete. But when concrete is subjected to shear stresses, a biaxial tension-compression stress field is induced. This reduces the peak compressive stress in concrete. Hence the uniaxial stress-strain relationships over estimates the force developed in concrete. To compensate for this, CFT neglects the concrete cover and hence reduces the moment arm thereby producing less force. Hence the shear flow zone is assumed to be entirely

contained inside the enclosed hoop reinforcement. This is based on the observation that the concrete at the corners of the cross section is under tension when subjected to torsional force. At high torsional forces the concrete will not have sufficient strength to prevent spalling. So the outside cross sectional dimensions are taken to the centerline of the transverse reinforcement.

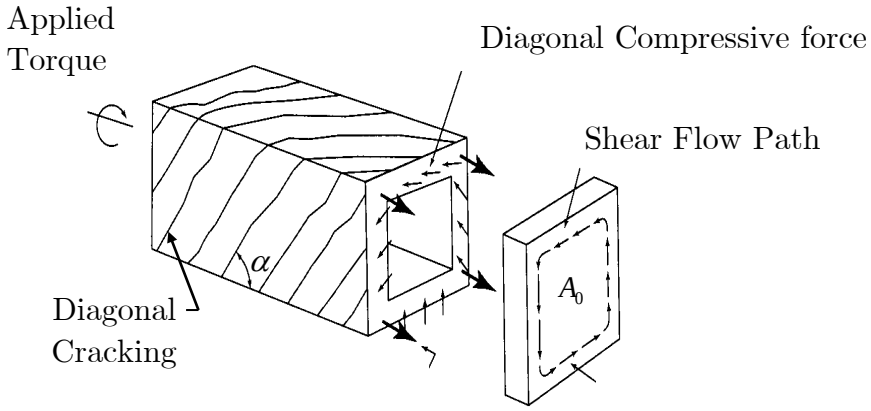

Figure 2.3. Cross section of shear panel and crack pattern developed under torsion [Reference. 1]

The basic concept of CFT is that it uses smeared or average values of stresses and strains. This is because the parameters mentioned changes in value along the depth of the cross section and hence is averaged and taken as constant across the depth of shear panel. Fig 2.3 shows the model of a shear panel. The angle of diagonal cracks α is taken as a variable in CFT. Limitations of CFT are:

- It neglects the compression softening of concrete under biaxial stresses.
- The tensile strength of concrete is neglected and hence can be applied only to post- cracking.

2.4. SOFTENED TRUSS MODEL (STM)

The model was developed by Hsu and Mo (1985). The basic concepts of Softened Truss Model and CFT are the same except for a few additional assumptions in STM for shear flow zone. The major difference is that STM incorporated compression softening of concrete under biaxial stresses. In STM the average stresses are assumed to occur at mid-depth of the shear flow zone as shown in Fig 2.4a. The area and perimeter of cross section are also calculated along the centerline of the shear flow zone. The STM defines failure at concrete crushing, which is assumed to occur when the principal compressive strain at the surface,ε_{ds}, reaches -0.0035 mm/mm. The equations for the compressive stress in softened concrete was developed by Vecchio and Collins in 1981 and later Hsu (1993) developed the formula for the softening coefficient. These equations shall be explained in detail in the forthcoming sections. The model however ignores the tension stiffening of concrete subjected to tension.

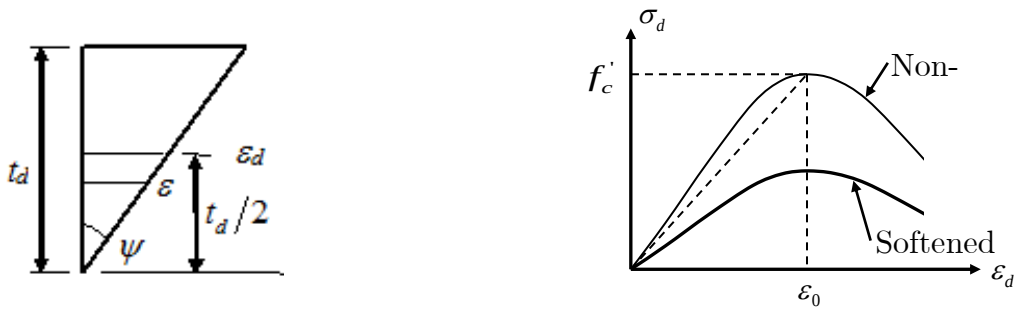

Figure 2.4 a) strain distribution b) Compression softening of concrete [Reference. 1]

In STM and CFT, the strains along the direction of a stress are solely generated by that stress. The strain generated by a stress acting in the normal direction due to the

Poisson effect is ignored. As a result, the truss models described above cannot accurately predict the post-peak response.

2.5. MODIFIED COMPRESSION FIELD THEORY (MCFT)

The model was developed by Mitchell and Collins for torsion and then later modified by Rahal and Collins (1995) for combined loading. The model is an improvisation of the Compression Field Theory. MCFT incorporates the softening behavior of concrete when subjected to biaxial stresses and also the tension stiffening of concrete when subjected to tensile forces.

The model idealizes the member to be composed of four wall panels instead of a single unit. The applied torsional moments and shear forces acts as shear stresses in each panel. It uses the strain compatibility conditions developed for CFT and also the equations for curvature of the concrete struts developed by Onsongo and Collins. The major difference between CFT and MCFT is the distribution of shear stresses along the shear flow zone. According to Bredt's thin tube theory, the shear stress due to torsion is assumed to act uniformly in the shear flow zone. But Rahal and Collins modified this statement by assuming a triangular distribution of shear stress caused by torsion over the thickness of shear flow zone. The shear stress induced due to shear force was assumed to act uniformly over the width of the tube. However they could not provide experimental justification for the above mentioned distribution of stresses.

2.6. TENSION STIFFENED SOFTENED TRUSS MODEL (TS-STM)

The TS-STM was developed by Gary Greene (2006), University of Missouri. The model is based on STM developed at the University of Houston. Here STM is revised to include the effect of concrete acting in tension known as tension stiffening. Concrete contributes to the tension capacity of the RC section even after cracking, but the tensile strength reduces drastically after cracking. The derivations will be explained in the next chapter. The strain compatibility equations are adopted from CFT. The torsion acting on the member is resisted by the shear stress acting uniformly over the shear flow zone as per Bredt's thin tube theory.

CHAPTER-3

COMBINED ACTION SOFTENED TRUSS MODEL

CHAPTER-3

COMBINED ACTION SOFTENED TRUSS MODEL

3.1. INTRODUCTION

The model was proposed to predict the load-deformation behaviour of a pre-stressed concrete member under torsion combined with bending and shear. The model was proposed by Greene (2006) and is an extension of TS-STM which was limited only to the case of pure torsion. The model idealizes a given member as equivalent panels subjected to shear and normal stresses. The process of division of a given section into equivalent panels are explained in the section 3.2. The effective thickness of each panel is equal to the depth of the shear flow zone in the panel. The definition of shear flow zone is explained in section 3.6. Equilibrium and strain compatibility is maintained in each panel. Longitudinal strain compatibility is maintained at the center of the member cross section. Warping in the panel induces bending in the concrete struts. The formulations developed so far are applicable only to rectangular sections (solid and hollow).

3.2. BASIC ASSUMPTIONS OF THE MODEL

The following are the assumptions made in the formulations of the CA-STM:

- The given rectangular member is divided into four walls, each of which can be idealized as RC shear panels.
- The external applied loads on the member are distributed to each of the panels as uniform normal and shear stresses.

- The truss model is used to model the RC member after cracking. i.e. the cracks separate the concrete into a series of diagonal struts that carry the compression and longitudinal and transverse reinforcements carry the tension or compression.
- Concrete contributes to the strength in compression in the diagonal struts and also tension in the perpendicular direction due to the stiffening action.
- The member is idealized to have only four shear panels and can be validated only for members subjected to bending along one axis combined with shear and torsion.
- Any member under torsion can be modeled as a thin tube as in Bredt's thin tube theory. In case of solid sections the core of the member does not contribute to the torsional resistance and hence neglected.
- The model neglects the dowel action of the reinforcement and assumes a perfect bond between concrete and reinforcement.
- They consider only in plane member stresses. Hence the bending moments and torsional moments should be distributed as shear and normal stresses in each panel.

3.3. MODEL CROSS SECTION

The cross section of the model is shown in Fig 3.1. The wall thickness of each panel of the original section is given by t_i where 'i' is the number of the wall panel. In case of a solid section the panel thickness is to be taken as $b/2$. The member is first idealized as a thin tube. The thickness of the thin tube is the thickness of the shear flow zone. This shall be denoted as t_d henceforth. The center line of the shear flow zone will form a rectangular section with dimensions h_0 and b_0. The panels are numbered as shown in Fig 3 .1 (c).

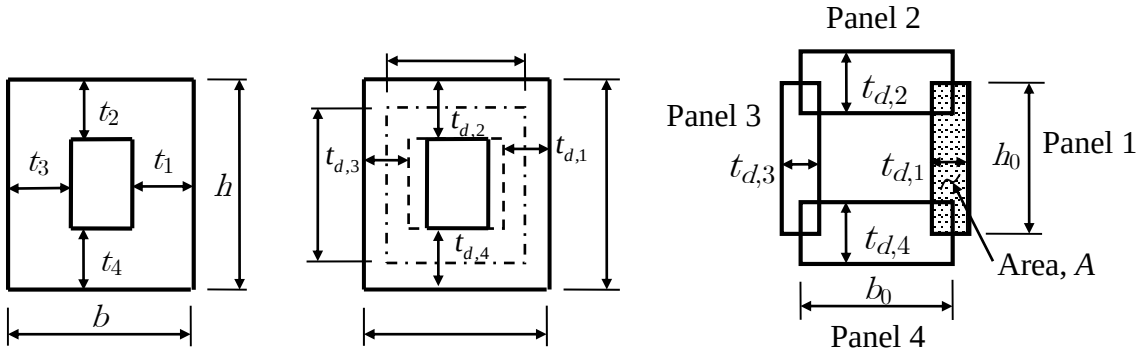

(a) Actual cross section (b) Thin tube model (c) Model cross section for CASTM

Figure 3.1 Model cross sectional details [Reference. 1]

3.4. BACKGROUND FOR THE DEVELOPMENT OF CA-STM

The behavior of an RC member under torsion differs significantly before and after cracking. Before cracking, the member is assumed to act homogeneous, and the shear stresses induced by the applied torque are resisted by the concrete alone. After diagonal cracks are formed the member is divided into a series of concrete struts, and hence the shear from the applied torque is resisted by a truss, with the concrete in

compression and the reinforcement in tension. Twisting in a non-circular member under torsion will also cause the initially plane surfaces to warp.

RC members before cracking is assumed as a homogeneous member. It is assumed to either behave elastically or plastically. Many theories were developed to predict the cracking torque and twist, (Bredt 1896; Hsu 1968). After cracking, the behavior was described by the truss models (Mitchell and Collins 1974; Hsu and Mo 1985a). Truss models assume that the wall of a member can be analyzed as a shear panel with the addition of a bending moment in the concrete struts due to warping. Therefore, an important part of understanding models for RC members under torsion is the modeling of RC panels under shear.

The analysis of shear panels includes the force equilibrium, strain compatibility and stress-strain relationships of concrete and reinforcement. The stress-strain relationship of concrete includes:

- Softening of concrete when subjected to biaxial tension compression field. i.e. concrete under biaxial tension and compression has stresses and strains significantly lower than those under uniaxial compression.
- Stiffening of concrete when subjected to tensile forces. The tension-stiffened response is related to the stress-strain response of concrete acting in tension.

3.5. BIAXIAL STRESS-STRAIN RELATIONSHIPS FOR CONCRETE

3.5.1. Compression softening

When a normal strength plain concrete is subjected to uniaxial compression, the simple parabolic model for concrete can be used. But the same cannot be used when the member is subjected to biaxial compression-tension stresses. In such cases the parabolic stress-strain response usually over estimates the capacity of the section. The compression softening of concrete was discovered by Robinson and Demorieux in 1972. Later many models were developed to accommodate these changes in the behavior of concrete. When RC panels are loaded under shear, it is subjected to biaxial tension-compression stress field. The compressive stress-strain response is different. Hence the parabolic stress-strain curve developed under uniaxial compression cannot be used. The model developed by Robinson and Demorieux scaled down the compressive stress with increase in strain. Their stress-strain relation is given by equation (2). The factors effecting the softening behavior could not be predicted by Robinson and Demorieux. The understanding of the behavior was studied in detail only when large scale testing of shear panels was made possible. The mathematical formulation for the various parameters controlling the softening was developed by Vecchio and Collins (1982) and Belarbi and Hsu (1991).

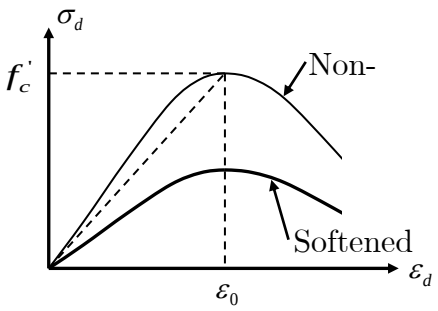

Figure 3.2 Softened stress-strain relationship for concrete in compression [Reference. 1]

The compressive stress given by parabolic model and softened model are given by equations (1) and (2).

$$\sigma_d = f_c' \left[2\left(\frac{\varepsilon_d}{\varepsilon_0}\right) - \left(\frac{\varepsilon_d}{\varepsilon_0}\right)^2 \right] \quad (1)$$

$$\sigma_d = k_1 \sigma_p \left[2\left(\frac{\varepsilon_d}{\varepsilon_0}\right) - \left(\frac{\varepsilon_d}{\varepsilon_0}\right)^2 \right] \quad (2)$$

In the above equations, f_c' is the compressive strength of concrete; ε_0 is the compressive strain at which peak compressive stress occurs; σ_p is the peak stress in the softened model. σ_p can be expressed as a function of f_c' and a softening coefficient, ζ. k_1 is a parameter that will be discussed in section 3.9.2. The expression is given by equation (3). The earliest expressions for ζ were proposed by Vecchio and Collins (1982) and Belarbi and Hsu (1991). The empirical relation given by Belarbi and Hsu has been adopted for the research. It is given by equation (4).

$$\sigma_p = \zeta f_c' \quad (3)$$

$$\zeta = \frac{0.9}{\sqrt{1+600\varepsilon_r}} \quad (4)$$

3.5.2. Tension Stiffening

Tension stiffened response is related to the stress-strain response of concrete loaded under tension. Early models based on Modified Compression Field Theory (MCFT) and Softened Truss Model (STM) neglects the tensile strength of concrete since they only have very small effect on the member's peak strength. Later it was observed that the tensile response of concrete has a significant effect on the member's load deformation response and hence cannot be neglected. The tension stiffened response of concrete is as shown below.

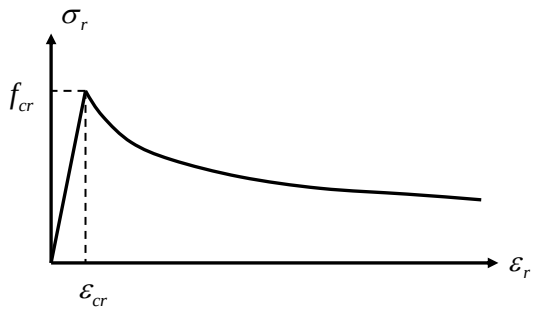

Figure 3.3 Average stress-strain response of concrete in tension [Reference. 1]

In case of a plain concrete member, the member behaves elastically when loaded under tension until the stress exceeds the tensile strength of concrete. After this point the concrete fails and the nature of failure is brittle. This is because the concrete cannot transfer tensile stresses across the cracks. The response in case of reinforced concrete is different after the stress exceeds the tensile strength of concrete. Once the cracks are formed perpendicular to the reinforcement, the steel carries the tensile stress. However, the stresses are still carried by concrete in between the cracks along with the reinforcement even though the contribution is very small. Thus the concrete

surrounding the reinforcement will add to the stiffness of the member. This phenomenon is known as tension stiffening. Therefore, it can be seen that the stress in reinforcement will be a maximum at the cracks and reduces to a minimum between the cracks. Similarly in concrete, the stresses are zero at the point of cracking and maximum in between the cracks.

3.5.2(a). Pre-Cracking: Before cracking, concrete can be assumed to obey Hooke's Law. Hence the ascending portion assumes a linear relationship and is given by equation (5). Here σ_r and ε_r are the average tensile stress and strain in concrete respectively. E_c is the modulus of elasticity of non-softened concrete. The equation is valid till σ_r becomes equal to f_{cr}. The expression for f_{cr} given by equation (6) was developed by Gary Greene(2006). In the expression A_g is the gross area of the cross section but it does not include the void of the cross section; A_{cp} is the total area inside the perimeter of the section; C is a constant whose value is derived to be 0.5 based on regression analysis. The sectional details are shown in Fig 3.4.

$$\sigma_r = E_c \varepsilon_r \tag{5}$$

$$f_{cr} = C \frac{A_g}{A_{cp}} \sqrt{f_c'} \tag{6}$$

$$A_{cp} = bh \tag{6a}$$

$$A_g = (b - t_4)t_1 + (h - t_1)t_2 + (b - t_2)t_3 + (h - t_3)t_4 \tag{6b}$$

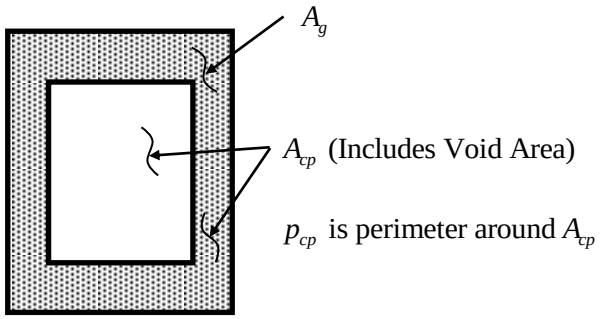

Figure 3.4. Sectional details for the calculation of cracking stress of concrete [Reference. 1]

3.5.2(b). Post–Cracking: The research uses the model developed by Greene (2006) to predict the post cracking behavior of RC members. He developed linear, parabolic and exponential relations to calculate stress-strain response after cracking. The parabolic expression is used because it provides a smooth transition between Softened Truss Model (STM) and Combined Action Softened Truss Model (CASTM). The expression is given by equation (7). In the equation for β_r, $\varepsilon_{cr0}$is the strain at which the tensile stress becomes zero. This value is taken to be 0.007. The variation is shown by Fig 3.5. ε_{cr} is the cracking strain of concrete which is approximately assumed to be 0.00014.

$$\sigma_r = f_{cr}(1 - 2\beta + \beta^2) \tag{7}$$

where

$$\beta_r = \frac{\varepsilon_r - \varepsilon_{cr}}{\varepsilon_{cro} - \varepsilon_{cr}} \tag{8}$$

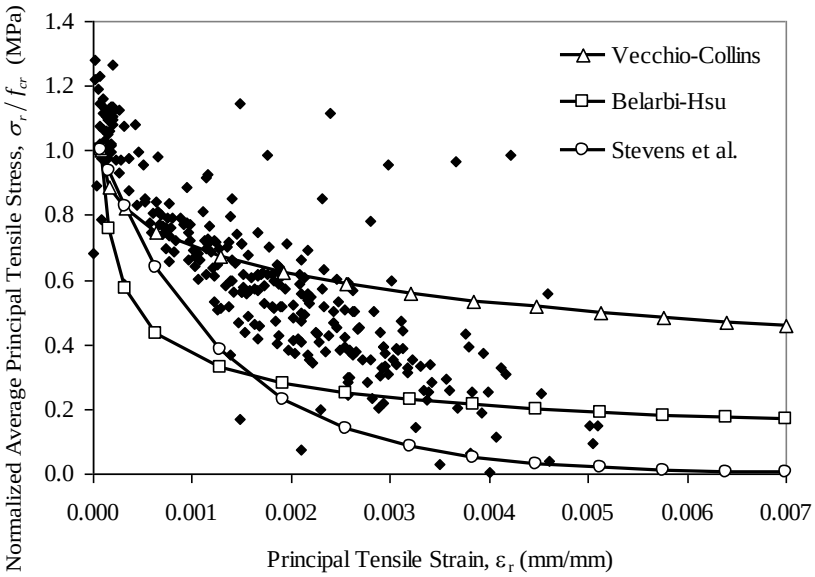

Figure 3.5 Normalized stress-tensile strain variation of concrete [Reference. 1]

3.6. STRESS-STRAIN RELATIONSHIPS OF REINFORCEMENT

The relationship for bare reinforcement is used in the CA-STM. An elastic-perfectly plastic model is used for predictions. E_s is the modulus of elasticity of steel, f_s is the stress acting on the reinforcement and f_{sy} is the yield stress of the reinforcement and ε_s is the strain developed in the steel. The following equations are used for both longitudinal and transverse reinforcements.

For $\varepsilon_s < 0.002$ $\quad f_s = E_s \varepsilon_s$ (9)

For $\varepsilon_s \geq 0.002$ $\quad f_s = f_{sy}$ (10)

3.7. BREDT'S THIN TUBE THEORY

When torsion acts on an RC member, it induces shear stress within the member. Bredt's thin tube theory is used to model the flow of shear stress over the cross section of an RC member when subjected to torsion. The main concept is to assume that the shear flows around the outside of the cross section. Hence the entire cross section of the member is idealized as a thin tube. The shear flow is assumed to be constant within the thin tube.

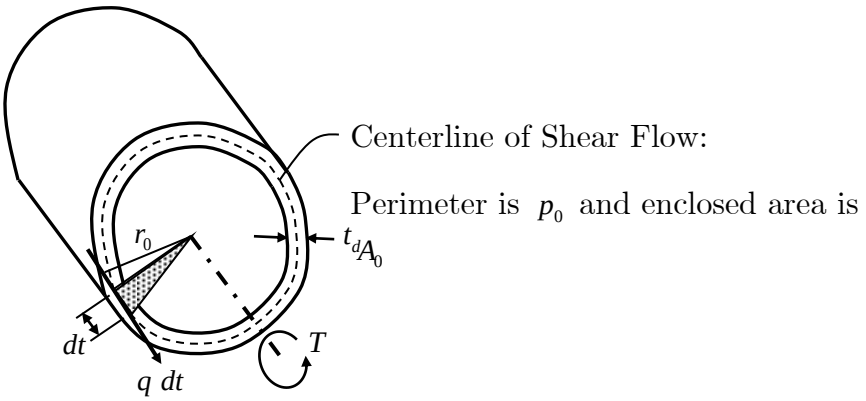

Figure 3.6 Representation of a thin tube under Torsion

In Bredt's thin tube theory, the constant shear stress τ, can be converted to a shear flow, q, by multiplying by the tube's thickness,h (i.e. $q = \tau \times h$). The shear stress circulating around the section develops an internal torque, T, given by Equation 11, where dt is the length of a wall element and r_0 is the moment arm from the centerline of the shear flow to the center of the twist. The product $r_0 dt$ is twice the area of the shaded triangle as shown in Fig 3.6. Integrating around the entire tube yields Equation [12], where A_0 is the area inside the shear flow centerline. Combining these two

equations yields Equation [13], a simple expression for the torque developed in a thin tube. An approximate thickness of the thin tube, or shear flow zone, is given by Equation [14].

$$T = q \int r_0 dt \tag{11}$$

$$\int r_0 dt = 2A_0 \tag{12}$$

Therefore,

$$T = 2A_0 q \tag{13}$$

$$t_d = \frac{3}{4}\frac{A_0}{p_0} \tag{14}$$

3.8. DISTRIBUTION OF APPLIED LOADS

The various forces acting in an RC member is shown in Fig 3.7. Since the model assumes that the member is subjected only to in-plane forces, the torsional and bending moments are converted into equivalent shear and normal stresses respectively. The stresses acts over the area of the thin tube within the section. The thickness over which the shear stresses act is known as the shear flow zone and is represented by t_d.

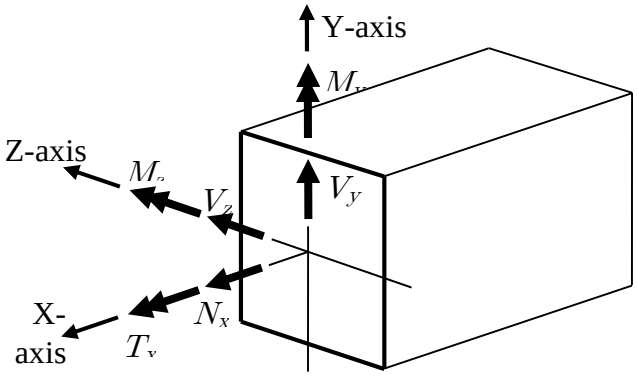

Figure 3.7. Generic Forces acting on the RC Section

As shown in Fig 3.7, the torsion applied induces a positive shear flow ,q $\left(q = \frac{T_x}{2A_0}\right)$. The flow is shown in Fig 3.8 (a). The shear stress due to the shear force flows parallel to the applied force. i.e. V_y $\left(q_y = \frac{V_y}{2h_0}\right)$ induces shear flow in panels 1 and 3. Similarly V_z $\left(q_z = \frac{V_z}{2b_0}\right)$ induces shear in panels 2 and 4. Since the shear due to both shear and torsion are assumed to be uniform over the shear flow zone, they can be summed up to get the net stresses acting on each panel. The net forces are shown in Fig 3.8 (b). The shear stress can be calculated by equation (19).

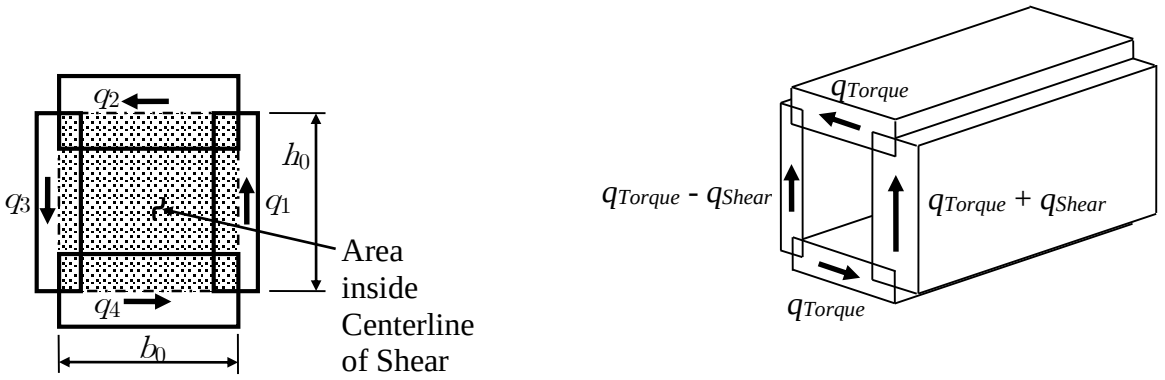

(a) Shear stress due to torsion (b) Net shear acting on each panel

Figure 3.8 Distribution of Shear force and Torsional moment in each panel

[Reference. 1]

$$q_1 = \frac{T_x}{2A_0} + \frac{V_y}{2h_0} \quad (15)$$

$$q_2 = \frac{T_x}{2A_0} + \frac{V_z}{2b_0} \quad (16)$$

$$q_3 = \frac{T_x}{2A_0} - \frac{V_y}{2h_0} \quad (17)$$

$$q_4 = \frac{T_x}{2A_0} - \frac{V_z}{2b_0} \quad (18)$$

$$\tau_{LT,i} = \frac{q_i}{t_{d,i}} \tag{19}$$

The applied bending moments and normal forces are distributed as normal stresses (σ_L) in the shear panels along the longitudinal axis of the member. The stresses are calculated such that the resultant normal force will generate a bending moment about the centerline of the member. The axial force can be derived by summing up the resultant forces on each panel. Equations (20), (21) and (22) gives the expressions for bending moments and axial force in terms of normal stress $\sigma_{L,i}$ of each panel.

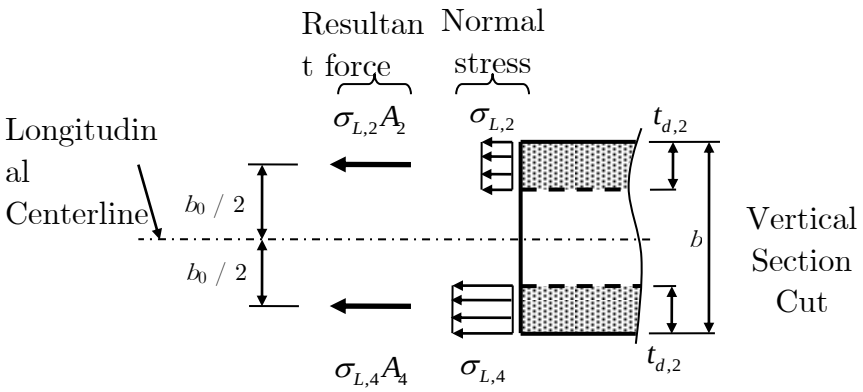

Figure 3.9 Distribution of bending moments and normal force in panels 2 and 4 [Ref:1]

$$M_y = [\sigma_{L,3}(t_{d,3}h_0) - \sigma_{L,1}(t_{d,1}h_0)]\left(\frac{b_0}{2}\right) \tag{20}$$

$$M_z = [\sigma_{L,4}(t_{d,4}b_0) - \sigma_{L,2}(t_{d,2}b_0)]\left(\frac{h_0}{2}\right) \tag{21}$$

$$N_x = \sigma_{L,1}(t_{d,1}h_0) + \sigma_{L,2}(t_{d,2}b_0) + \sigma_{L,3}(t_{d,3}h_0) + \sigma_{L,4}(t_{d,4}b_0) \tag{22}$$

3.9. EQUILIBRIUM AND STRAIN COMPATIBILITY

Equilibrium and strain compatibility is maintained in each panel. The longitudinal direction in the panel (L-axis) is aligned to be parallel to the centerline of the member,

and the transverse direction of the panel (T-axis) is aligned to be perpendicular to the member's centerline. The proposed model assumes a wall panel has an orthogonal grid of reinforcement in L and T directions and has cracks at an angle α to the L -axis. . The cracks are normal to the principal tensile stress, and the principal tensile and compressive stresses act in the d and r directions.

The alignment of the axes are shown in Fig 3.10. The cracks divide the panel into a series of concrete struts, which allows the panel to act as a truss such that the concrete is under compression and the reinforcement is under tension or compression. The model includes three equilibrium equations and the three compatibility equations for an RC panel under in-plane membrane stresses. The Equilibrium and strain compatibility equations are given in the equations (23) to (28). $A_{L,i}$ is the area of longitudinal reinforcement in each panel and A_T is the transverse reinforcement.

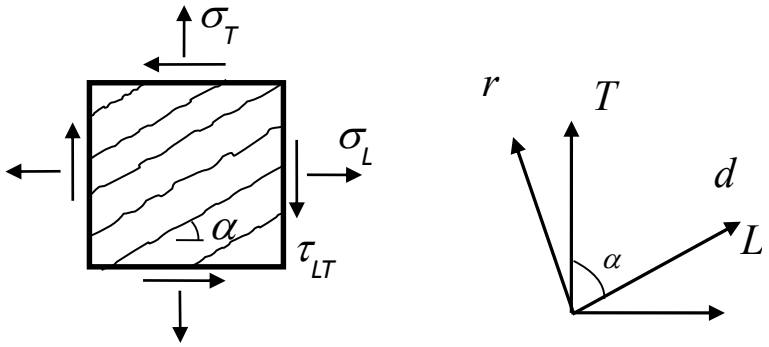

Figure 3.10 RC membrane element with the coordinate axes [Reference. 3]

$$\sigma_{L,i} = \sigma_{d,i}cos^2\alpha_i + \sigma_{r,i}sin^2\alpha_i + f_{L,i}\left(\frac{A_{L,i}}{t_{d,i}p_0}\right) \quad (23)$$

$$\sigma_{T,i} = \sigma_{d,i}sin^2\alpha_i + \sigma_{r,i}cos^2\alpha_i + f_{T,i}\left(\frac{A_T}{t_{d,i}s}\right) \quad (24)$$

$$\tau_{LT,i} = \left(-\sigma_{d,i} + \sigma_{r,i}\right) sin\alpha_i cos\alpha_i . sign(q_i) \quad (25)$$

$$\gamma_{LT,i} = 2\left(-\varepsilon_{d,i} + \varepsilon_{r,i}\right) sin\alpha_i cos\alpha_i . sign(q_i) \quad (26)$$

$$\varepsilon_{L,i} = \varepsilon_{d,i} cos^2\alpha_i + \varepsilon_{r,i} sin^2\alpha_i \quad (27)$$

$$\varepsilon_{T,i} = \varepsilon_{r,i} + \varepsilon_{d,i} - \varepsilon_{L,i} \quad (28)$$

3.10. STRESS-STRAIN DISTRIBUTION IN CONCRETE

3.10.1. Strain Distribution:

The model assumes that the shear stress (τ_{lt}) due to shear force and torsion acts uniformly over the thickness of the shear flow zone given by Bredt's thin tube theory. The strain distribution is as given below in Fig 3.11. The principal compressive strain at the exterior surface of concrete is given by $\varepsilon_{ds,i}$ and the principal compressive strain at half the depth of t_d is given by $\varepsilon_{d,i}$ in the given figure.

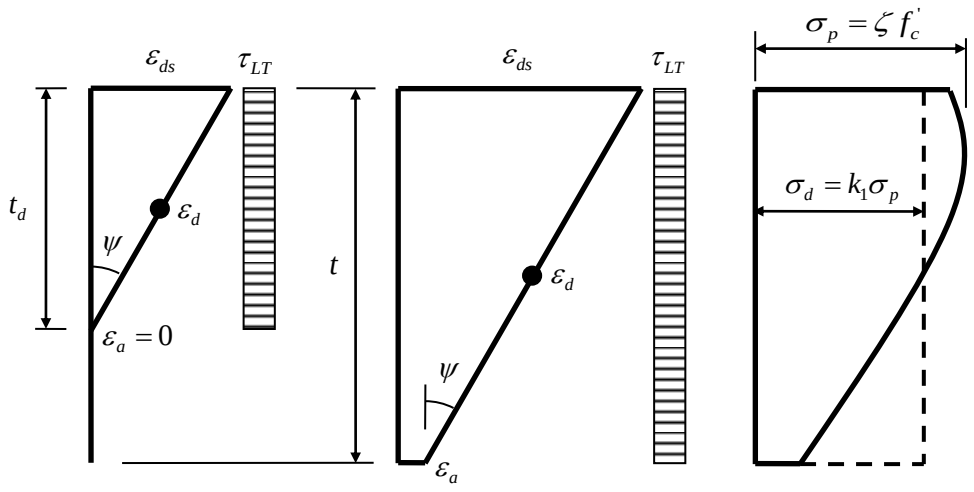

(a) $t_d < t_i$ (b)$t_d = t_i$ (c) average stress distribution

Figure 3.11. Shear Stress and strain distribution in concrete over the shear flow zone

[Reference. 1]

When $t_d < t_i$ as in Fig 3.11 (a), the compressive strain, ε_a will reduce to zero at the depth of shear flow zone. But when the depth of shear flow zone is equal to the thickness of the wall, there will be the presence of a compressive strain at t_d. $\varepsilon_{d,i}$ is calculated as the average of ε_a and $\varepsilon_{ds,i}$. Equation (30) gives the expression to calculate the curvature in each panel.

$$\varepsilon_{d,i} = \frac{(\varepsilon_{ds,i}+\varepsilon_{a,i})}{2} \tag{29}$$

$$\Psi_i = \frac{-(\varepsilon_{ds,i}-\varepsilon_{a,i})}{t_{d,i}} \tag{30}$$

3.10.2. Stress Distribution:

The model uses the concept of smeared stresses or average stresses similar to STM. The stress distribution in the concrete strut is as shown in Fig 3.11 (c). The average stress is calculated as per equation (2), where k_1 is the ratio of average stress to peak stress in the respective panels considered. The equations for k_1 are given by (31a) and (31b).

For $\varepsilon_{a,i} < \varepsilon_{ds,i}$

$$k_{1,i} = \left[\frac{\varepsilon_{ds,i}}{\varepsilon_0}\left(1-\frac{\varepsilon_{ds,i}}{3\varepsilon_0}\right) - \frac{\varepsilon_{a,i}^2}{\varepsilon_{ds,i}\varepsilon_0}\left(1-\frac{\varepsilon_{a,i}}{3\varepsilon_0}\right)\right]\left(\frac{\varepsilon_{ds,i}}{\varepsilon_{ds,i}-\varepsilon_{a,i}}\right) \tag{31a}$$

For $\varepsilon_{a,i} = \varepsilon_{ds,i}$

$$k_{1,i} = \frac{(2\varepsilon_{ds,i}\varepsilon_0-\varepsilon_{ds}^2)}{\varepsilon_0^2} \tag{31b}$$

3.11. STRAIN COMPATIBILITY AMONG PANELS

The strain compatibility in panels are maintained by several conditions. The longitudinal strains are related to the strain along the center line of the member. The panels develop longitudinal and transverse curvature and these in addition to the member's twist, contributes to the total curvature of each panel.

3.11.1. Longitudinal and Transverse curvature in panels:

The normal strains in the longitudinal and transverse directions of each panel, $\varepsilon_{L,i}$ and $\varepsilon_{T,i}$, are calculated using Equations (27) and (28). The difference in longitudinal strain between Panels 1 and 3 causes the curvature about member's y-axis which is given by $\boldsymbol{\varphi_{L,13}}$. Also, the difference in transverse strain between the these two panels causes a transverse curvature, $\boldsymbol{\varphi_{T,13}}$, about the member's z-axis. Fig 3.12 shows these curvatures. The difference between the longitudinal and transverse strain in Panels 2 and 4 causes the curvatures $\boldsymbol{\varphi_{L,24}}$ and $\boldsymbol{\varphi_{T,24}}$. The equations for transverse curvatures are given by equations (32) and (33). The longitudinal curvatures can also be calculated similarly.

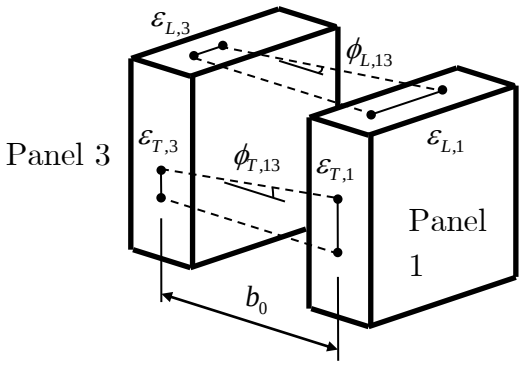

Figure 3.12 longitudinal and transverse curvatures in panels 1 and 3 [Reference. 1]

$$\varphi_{T,13} = \frac{(\varepsilon_{T,1} - \varepsilon_{T,3})}{b_0} \tag{32}$$

$$\varphi_{T,24} = \frac{(\varepsilon_{T,2} - \varepsilon_{T,4})}{b_0} \tag{33}$$

3.11.2. Longitudinal strain compatibility among panels:

The section is idealized as a thin tube and the strain at the center of the tube is given by ε_{CL}. The longitudinal strains in each panel are then correlated with the center line strain and the longitudinal curvatures. The longitudinal strain is calculated long the center line of each panel.

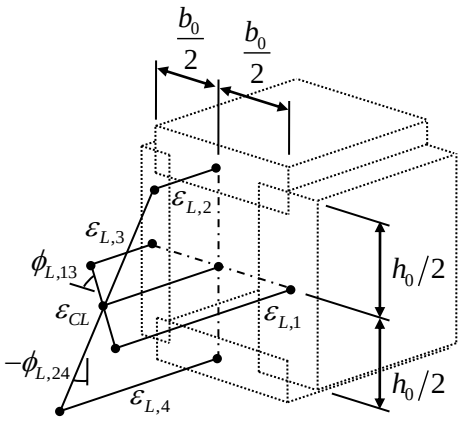

Figure 3.13 Longitudinal strain compatibility [Ref. 1]

$$\varepsilon_{L,1} = \varepsilon_{CL} + \varphi_{L,13}\left(\frac{b_0}{2}\right) \tag{34a}$$

$$\varepsilon_{L,2} = \varepsilon_{CL} + \varphi_{L,24}\left(\frac{h_0}{2}\right) \tag{34b}$$

$$\varepsilon_{L,3} = \varepsilon_{CL} - \varphi_{L,13}\left(\frac{b_0}{2}\right) \tag{34c}$$

$$\varepsilon_{L,4} = \varepsilon_{CL} - \varphi_{L,24}\left(\frac{h_0}{2}\right) \tag{34d}$$

3.11.3. Twist on concrete strut:

For a closed section, the total warping displacement around the perimeter must be zero. The expression for twist can be derived by relating it to the shear strain in each panel. The shear strain in a panel is taken to be a constant. Equation (35) gives the expression for twist under combined loading in a rectangular section

$$\theta = \left[\left(\gamma_{LT,1} + \gamma_{LT,3}\right)h_0 + \left(\gamma_{LT,2} + \gamma_{LT,4}\right)b_0\right]\frac{1}{2A_0} \qquad (35)$$

3.11.4. Curvature of concrete strut:

The compressive strut is inclined to the direction of principal compressive stress at an angle equal to α. The curvature in a compressive strut depends on curvature along longitudinal and transverse directions, $\varphi_{L,i}$ and $\varphi_{T,i}$ as well as the angle of twist θ, of the member given by equation (35). The curvature in the wall panel and concrete strut is shown in Fig 3.14. In a rectangular member, the exterior surface of the wall is a plane surface before twisting. As a torsional moment is applied, the wall becomes a hyperbolic surface. The warping causes a maximum curvature in the wall equal to the member's unit twist, θ, along a plane inclined 45° from the member's longitudinal axis as shown in Fig 3.14. In Panel 1, the transverse curvature will be a maximum along the side of the panel and the longitudinal curvature will be a maximum along the top of the panel as shown in Fig 3.14.

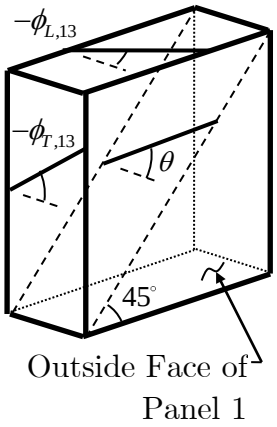

Figure 3.14 curvature in concrete strut [1]

The curvature due to, $\varphi_{L,i}, \varphi_{T,i}$, and θ can be calculated along any inclined plane using Mohr's circle. The equation for curvature is given by equation (36).

$$\Psi_1 = \theta sin2\alpha_1 - (\varphi_{L,13})cos^2\alpha_1 - (\varphi_{T,13})sin^2\alpha_1 \quad (36a)$$

$$\Psi_2 = \theta sin2\alpha_2 - (\varphi_{L,24})cos^2\alpha_2 - (\varphi_{T,24})sin^2\alpha_2 \quad (36b)$$

$$\Psi_3 = \theta sin2\alpha_3 + (\varphi_{L,13})cos^2\alpha_3 + (\varphi_{T,13})sin^2\alpha_3 \quad (36c)$$

$$\Psi_4 = \theta sin2\alpha_4 + (\varphi_{L,24})cos^2\alpha_4 + (\varphi_{T,24})sin^2\alpha_4 \quad (36d)$$

3.12. SHEAR FLOW ZONE INDEX ($\mathbf{Z_i}$)

The geometry of the shear flow zone is described using the variables $\varepsilon_{ds,i}, \varepsilon_{a,i}, \Psi_i, \varepsilon_{d,i}, t_{d,i}$ and t_i. The variables $t_{d,i}$ and $\varepsilon_{a,i}$ can be defined by the depth into the wall (for $t_d < t$) or the distance along the inside surface (for $t_d = t$). Point a is defined as the depth into the member where the principal compressive strain is zero when $t_d < t$ or the point where the strain profile intersects the inside surface of the wall for $t_d = t$ as shown in Fig. 3.15. An index z_i, is introduced to describe the location of a. The variables $t_{d,i}$ and $\varepsilon_{a,i}$ can then be expressed in terms of z_i.

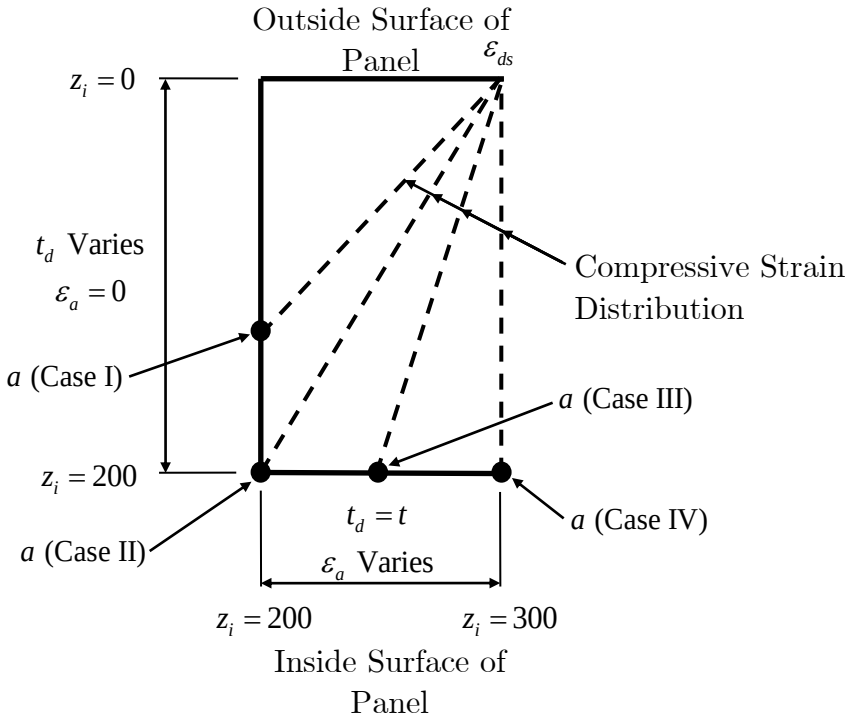

Figure 3.15 shear flow zone index with variation of strain distribution [Reference. 1]

The index z_i can vary from 0 to 300. For Case I, $t_d < t$ and z_i varies from 0 to 200, and the distance from the outside surface to point a is proportional to the value of z_i . For this case, $t_{d,i}$ is proportional to z_i and $\varepsilon_{a,i}$ equals zero. A value of 200 for z_i (Case II) indicates that $t_d = t$ and $\varepsilon_{a,i}$ equals zero. For Case III, a is located along the inside surface and $t_d = t$. The index z_i varies from 200 to 300, and $\varepsilon_{a,i}$ increases as a linear function of z_i until $\varepsilon_{a,i} = \varepsilon_{ds,i}$Case IV occurs when z_i equals 300 and $\varepsilon_{a,i} = \varepsilon_{ds,i}$ indicating a uniform strain in the compressive strut. Expressions for $t_{d,i}$ and $\varepsilon_{a,i}$ are given by Equations (37) and (38), and Fig 3.15 illustrates the four cases for a as described previously.

For $0 < z_i \leq 200$

$$t_{d,i} = z_i \left(\frac{t_i}{200}\right) \quad (37a)$$

$$\varepsilon_{a,i} = 0 \quad (38a)$$

For $200 < z_i \leq 300$

$$t_{d,i} = t_i \quad (37b)$$

$$\varepsilon_{a,i} = (z_i - 200) \left(\frac{\varepsilon_{ds,i}}{100}\right) \quad (38b)$$

3.13. DISTRIBUTION OF LONGITUDINAL REINFORCEMENT

An important consideration in idealizing the walls of a member as panels is the method used to distribute the longitudinal reinforcement.

- Symmetric reinforcement: In a member where the longitudinal reinforcement is symmetrically arranged around the cross section, the total area of reinforcement is distributed equally into each wall panel.
- Asymmetric reinforcement: The method used to distribute the longitudinal reinforcement in a member with an asymmetric arrangement is more complex. A portion of the total cross-sectional area of the longitudinal reinforcement must be distributed to each wall panel. The method developed was to distribute equal areas to each panel. The method was chosen for the CA-STM because equal area distribution is inherently used in the TS-STM for the case of a member under pure torsion with symmetrical reinforcement. By using the equal area method in the CA-STM, the predictions of load-deformation behavior made by the TS-STM and CA-STM should

be similar for this case. Fig 3.16 shows the idealization for distribution of longitudinal reinforcement.

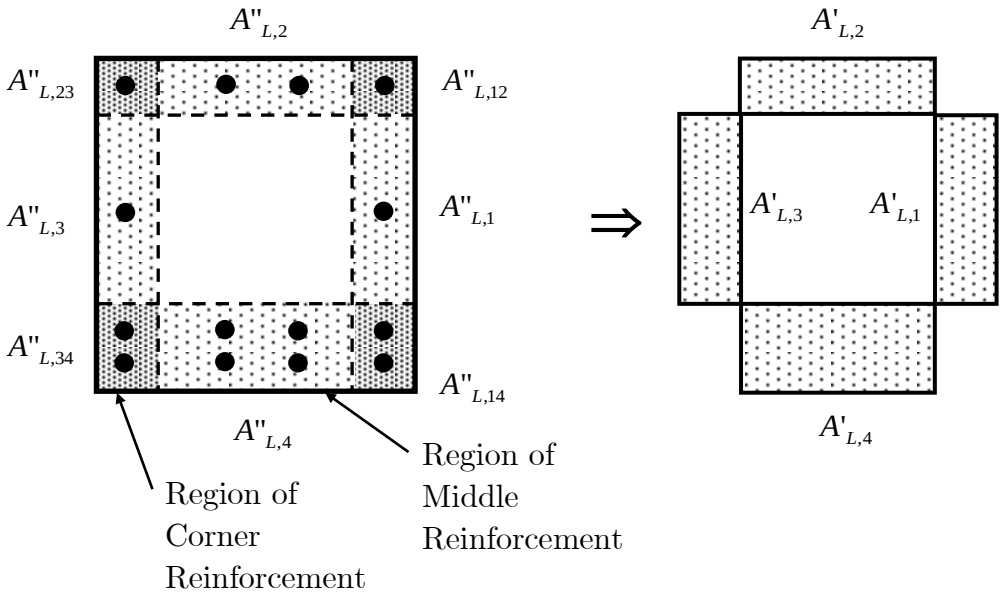

Figure 3.16 Idealization of RC section for distribution of longitudinal reinforcement [Reference. 1]

Assuming uniform stress in reinforcement, the bottom wall has more reinforcement and can generate more force in its longitudinal steel than in the top wall with less reinforcement, as shown in Fig 3.17.

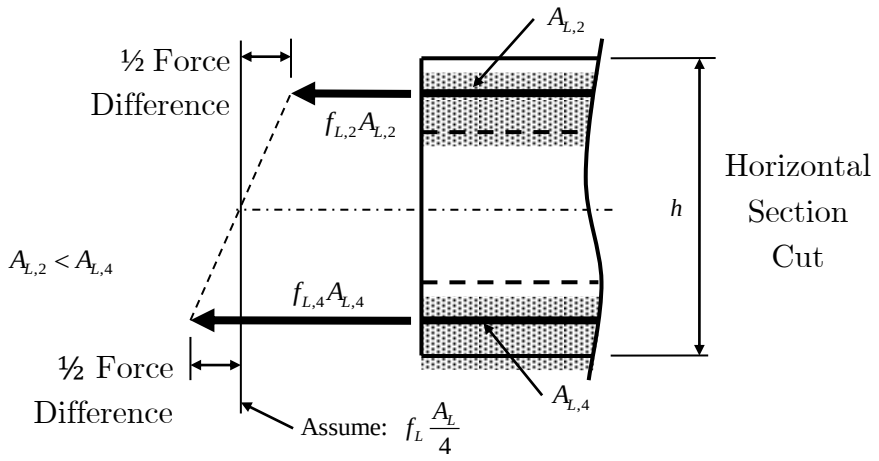

Figure 3.17 Equal force assumption for distribution of longitudinal reinforcement [Reference. 1]

The force in the two side walls would then be equal to the average of the force in the top and bottom walls. Based on the uniform stress concept, the average of the reinforcement in the top and bottom walls, which is equal to one-quarter of the total area of longitudinal reinforcement, would need to be distributed to each side wall. The reinforcement in the bottom and top walls is then one-quarter of the total area of longitudinal reinforcement, plus or minus half the difference in reinforcement, respectively. The corner reinforcement is distributed into the middle regions of the four panels and are given by the equations 39(a) to 39(d). Then the middle reinforcements are again distributed to the four panels as given by equations 40(a) to 40(d).

$$A'_{L,1} = \frac{1}{2}A"_{L,1} + \frac{1}{2}\left(A"_{L,12} + A"_{L,14}\right) \qquad 39(a)$$

$$A'_{L,2} = \frac{1}{2}A"_{L,2} + \frac{1}{2}\left(A"_{L,12} + A"_{L,23}\right) \qquad 39(b)$$

$$A'_{L,3} = \frac{1}{2}A"_{L,3} + \frac{1}{2}\left(A"_{L,23} + A"_{L,34}\right) \qquad 39(c)$$

$$A'_{L,4} = \frac{1}{2}A"_{L,4} + \frac{1}{2}\left(A"_{L,14} + A"_{L,34}\right) \quad 39(d)$$

$$A_{L,1} = \frac{A_L}{4} + \frac{1}{2}\left(A'_{L,1} - A'_{L,3}\right) \quad 40(a)$$

$$A_{L,2} = \frac{A_L}{4} + \frac{1}{2}\left(A'_{L,2} - A'_{L,4}\right) \quad 40(b)$$

$$A_{L,3} = \frac{A_L}{4} + \frac{1}{2}\left(A'_{L,3} - A'_{L,1}\right) \quad 40(c)$$

$$A_{L,4} = \frac{A_L}{4} + \frac{1}{2}\left(A'_{L,4} - A'_{L,2}\right) \quad 40(d)$$

3.14. ADDITIONAL EQUATIONS

The angle α_i is eliminated from the equilibrium equations by expressing it in terms of $\varepsilon_{d,i}$, $\varepsilon_{r,i}$, $\varepsilon_{L,i}$ and $\varepsilon_{T,i}$ in each panel. This is given by equations (41) and (42). The direction of spirals caused by positive T_x is considered as the positive direction of α_i.

$$cos^2\alpha_i = \frac{\varepsilon_{r,i} - \varepsilon_{L,i}}{\varepsilon_{r,i} - \varepsilon_{d,i}} \quad (41)$$

$$sin^2\alpha_i = \frac{\varepsilon_{L,i} - \varepsilon_{d,i}}{\varepsilon_{r,i} - \varepsilon_{d,i}} \quad (42)$$

The variables describing the shear flow zone are A_0, p_0, b_0 and h_0 and are given by equations (43),(44), (45) and (46).

$$A_0 = b_0 h_0 \quad (43)$$

$$P_0 = 2(b_0 + h_0) \quad (44)$$

$$b_0 = b - \left(\frac{t_{d,1} + t_{d,3}}{2}\right) \quad (45)$$

$$h_0 = h - \left(\frac{t_{d,2} + t_{d,4}}{2}\right) \quad (46)$$

3.15. METHOD OF SOLUTION OF CA-STM

The total number of unknown variables in the equations derived for the CA-STM exceeded the total number of CA-STM equations by six. This means that six variables needed to be selected and then the remaining variables could be solved using the equations of the CA-STM. For example, a purely "force-controlled" procedure could be used where all six possible loads could be specified ($\boldsymbol{T_x}$, $\boldsymbol{V_y}$, $\boldsymbol{V_z}$, $\boldsymbol{M_y}$, $\boldsymbol{M_z}$ and $\boldsymbol{N_x}$). However, this approach could cause difficulties in finding a solution if the selected loads were greater than the peak loads that could be predicted by the CA-STM. Another problem in using a force-controlled procedure is that two possible solutions could be found for the same selected loads: one pre-peak and one post-peak. Alternately, a purely "displacement-controlled" solution could be used and six variables relating to strain or displacement could be specified. However, the loads predicted by this method would be arbitrary and would make using and validating the model difficult.

The method of solution developed for the CA-STM uses a combination of the force-controlled and displacement-controlled methods described previously and allows the model to calculate predicted load-deformation responses under specified ratios of torque to bending, shear, and axial load.

The following algorithm solves the system of equations comprising the CA-STM for one point on the load-deformation response curve. The entire response from zero torque to the peak torque can be calculated by varying $\boldsymbol{\varepsilon_{ds,i}}$ from near zero to a limiting value that causes the peak torque, or that causes $\boldsymbol{\varepsilon_{ds,i}}$ to exceed 0.0035 mm/mm, whichever is smaller. An $\boldsymbol{\varepsilon_{ds,i}}$ value of 0.0035 mm/mm or greater is defined as the ultimate concrete compression strain.

3.15.1. SOLUTION PROCEDURE

Given:

- *Cross sectional details:* height (h), breadth (b) and thickness of each wall (t_i).
- *Reinforcement details:* Area of longitudinal reinforcement ($A_{L,i}$), area of transverse reinforcement (A_T) and spacing of transverse reinforcement (s).
- *Reinforcement material properties:* f_{Ly}, f_{Ty} and E_s.
- *Concrete material properties:* f'_c, ε_0, ε_{cr} and ε_{cr0}.

Initial Calculations:

The calculations of those variables that are constant throughout the process are made in this step of the solution procedure. It includes the cross sectional calculations (A_{cp}, A_g) and calculating the concrete cracking stress (f_{cr}, E_c) and yield strains ($\varepsilon_{Ly}, \varepsilon_{Ty}$) using equations (6a), (6b), (6), (5) and (10).

Solution Algorithm:

i. Select a value of $\varepsilon_{ds,i}$ and the ratios of M/T_x, V/T_x and N/T_x.

ii. Assume values of ε_{CL}, $\varphi_{L,13}$ and $\varphi_{L,24}$.

iii. Assume values of $\varepsilon_{ds,2}$, $\varepsilon_{ds,3}$, $\varepsilon_{ds,4}$ and T_x. Then calculate the forces and moments from the assumed ratios in step (i).

iv. Assume the value of θ.

v. Assume values of $\varepsilon_{r,i}$ and z_i.

vi. Calculate the shear flow zone parameters (A_0, p_0, b_0 and h_0) using equations (43), (44), (45), and (46) resp., Stresses in reinforced concrete ($\sigma_{d,i}$, $\sigma_{p,i}$, k_1, ζ) using equations (2), (3), (31a), (31b) and (4) resp., strains $\varepsilon_{a,i}$, $\varepsilon_{d,i}$, $\varepsilon_{L,i}$ and $\varepsilon_{T,i}$ using equations (38a), (38b), (29), (34a), (34b), (34c), (38a), and (28). Then calculate $\sigma_{T,i}$ using equation (24). Then calculate Ψ_i from equations (30) and (36a), (36b), (36c) and (36d).

vii. Compare Ψ_i obtained from (30) and (36). If the difference is not within the tolerable limit, adjust the value of z_i and repeat the steps v to vii until convergence is obtained. If the value of $\sigma_{T,i}$ is not close to zero within a tolerable limit, modify the value of $\varepsilon_{r,i}$ and repeat the steps v through vii until convergence is obtained.

viii. Calculate $\gamma_{LT,i}$ and θ from Equations (26) and (35). If the difference between the assumed and calculated value of θ is not within a tolerable limit, then adjust the assumed value and repeat Steps iv through viii until convergence is obtained.

ix. Calculate q_i from Equations (15), (16), (17) and (18) and $\tau_{LT,i}$ from Equations (19) and (25). If the difference between the two values for $\tau_{LT,i}$ is not within a tolerable limit for Panels 2, 3, and 4, then adjust the assumed values of and $\varepsilon_{ds,2}$, $\varepsilon_{ds,3}$ and $\varepsilon_{ds,4}$ and repeat Steps iii through ix until convergence is obtained. Also, if the difference between the two values for $\tau_{LT,i}$ is not within a tolerable limit for Panel 1, then adjust the assumed value of T_x and repeat Steps iii through ix until convergence is obtained.

x. Calculate$f_{L,i}$, $\sigma_{L,i}$, M and N from Equations (10), (23), (20), (21) and (22). If the difference between the calculated and selected values of M and N are not within a tolerable limit, then adjust the assumed values of φ_L and ε_{CL} respectively, and repeat Steps ii through x until convergence is obtained.

xi. Calculate α_i.

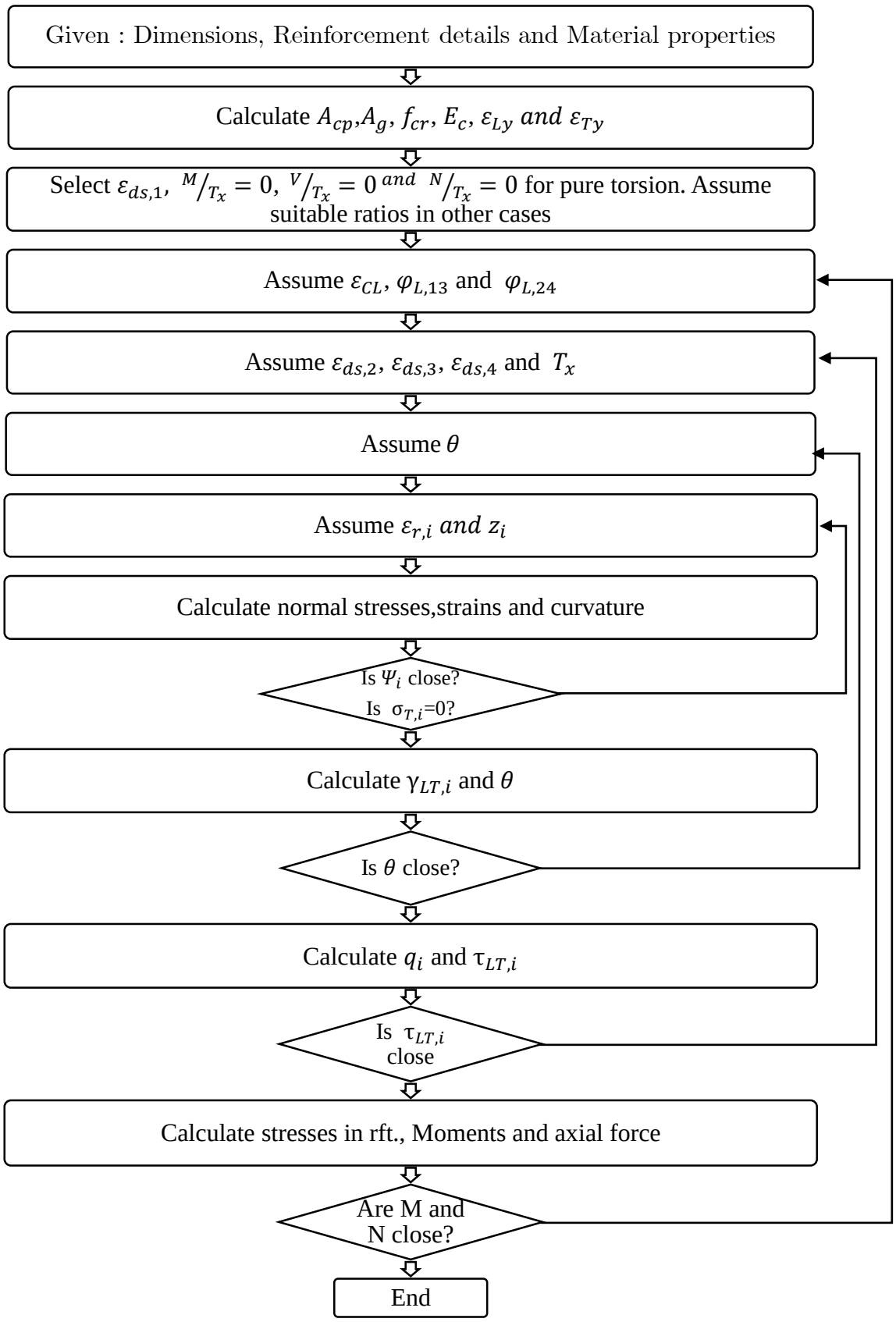
Given : Dimensions, Reinforcement details and Material properties
Calculate A_{cp},A_g, f_{cr}, E_c, ε_{Ly} and ε_{Ty}
Select $\varepsilon_{ds,1}$, $^{M}/_{T_x} = 0$, $^{V}/_{T_x} = 0$ ^{and} $^{N}/_{T_x} = 0$ for pure torsion. Assume suitable ratios in other cases
Assume ε_{CL}, $\varphi_{L,13}$ and $\varphi_{L,24}$
Assume $\varepsilon_{ds,2}$, $\varepsilon_{ds,3}$, $\varepsilon_{ds,4}$ and T_x
Assume θ
Assume $\varepsilon_{r,i}$ and z_i
Calculate normal stresses,strains and curvature
Is Ψ_i close?
Is $\sigma_{T,i}$=0?
Calculate $\gamma_{LT,i}$ and θ
Is θ close?
Calculate q_i and $\tau_{LT,i}$
Is $\tau_{LT,i}$ close
Calculate stresses in rft., Moments and axial force
Are M and N close?
End

CHAPTER-4

VALIDATION OF RESULTS AND DISCUSSION

CHAPTER-4

VALIDATION OF RESULTS AND DISCUSSION

4.1. INTRODUCTION:

The CA-STM can predict the full load-deformation response of reinforced concrete and pre-stressed concrete members under torsion combined with other loading actions. The model gives predictions of twist, concrete and reinforcement strain, and curvature from before cracking up to peak torque. The CA-STM model was formulated following the given algorithm in Matlab. The developed model was then validated for various cases of combined loads. The load combinations used are mentioned below:

4.1(a). Pure Torsion: The specimens tested by Lampert and Thurliman and McMullen and Warwaruk were used for the validations. The specimens differed in their cross sectional details and material properties. All the specimens chosen had hollow sections.

4.1(b). Torsion combined with Shear: The shear force applied on the member is expressed as a fraction of the applied torsion. Rahal and Collins conducted experimental studies on RC members subjected to combined torsion and shear. These results were used for the validation of CA-STM under the same load combination. The validations for different ratios of Torque to shear (T/V) are presented in section 4.3.

4.1(c). Torsion combined with shear, bending and axial force: All the loads acting on the member is expressed as a fraction of the applied torsion. The specimens tested by Tirasit is used for the validation of results. Four specimens were chosen. All the specimens had same cross sectional details. They only differed in the ratio of

applied torque to moment (T/M) and torque to lateral force (T/V). The validation for each of the above mentioned cases are explained in sections 4.2, 4.3 and 4.4.

4.2. RESPONSE OF MEMBERS UNDER PURE TORSION

4.2.1. McMullan and Warwaruk Specimens:

McMullan and Warwaruk tested RC specimens under pure torsion. The testing was done for two series each having the same cross sectional dimensions of 150mm x 300mm and a wall thickness of 45mm each. The length of the specimens were 3.0 m. The compressive strength of concrete used was 34 MPa and the yield strength of steel used was 360 MPa.

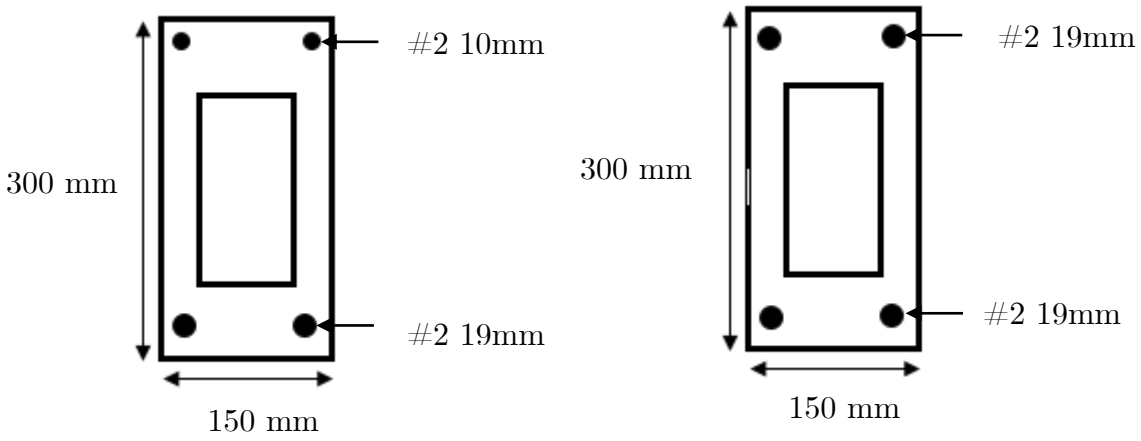

Figure 4.1 Cross sectional details of McMullan and Warwaruk Specimens

Table 4.1 Cross Sectional Details of McMullen and Warwaruk Specimen

Cross sectional dimensions : B = 150 mm, H = 300 mm			
series	Top steel (long.)	Bottom steel (long)	Transverse steel
1	#2 10mm	#2 19mm	10mm @ 83mm c/c
2	#2 19mm	#2 19mm	10mm @83mm c/c

The results obtained for the torque-twist behavior of series 1 and series 2 by the developed model for CASTM are in good agreement with the experimental results obtained by McMullen and Warwaruk. Series 2 with higher reinforcement at top showed an improvement by 35% in the experimental studies. The same could not be predicted by CA-STM which showed only an increase by 15%. The degree of rotation was predicted with higher accuracy to the experimental data.

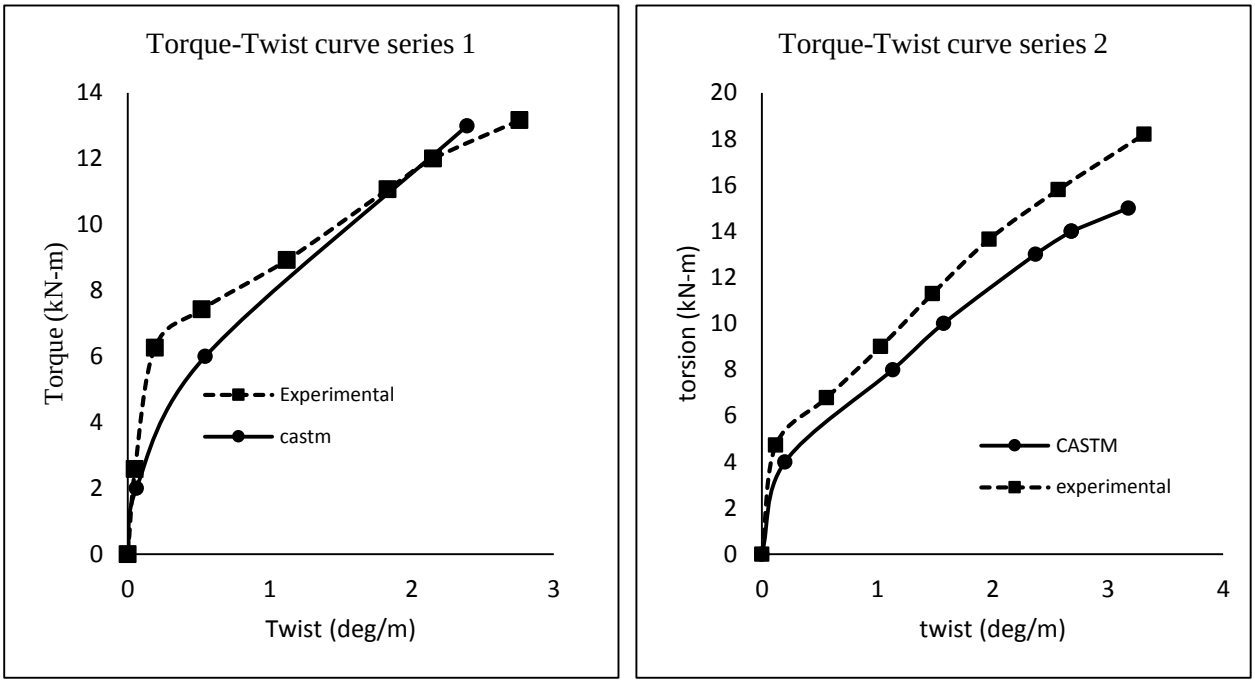

(a) Series 1 (b) Series 2

Figure 4.2: Validation of Improved CASTM with Experimental Data under Pure Torsion

4.2.2. Lampert and Thurliman Specimens:

The testing was done for square specimen with a wall thickness of 80mm each. The length of the specimens were 3.9 m. The concrete compressive strength was 26 MPa and the yield strength of steel used was 390 MPa.

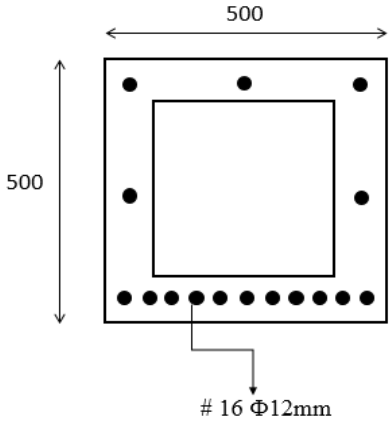

Figure 4.3 Cross Sections of Lampert and Thurliman Specimens

Table 4.2 Cross Sectional Details of Lampert and Thurliman Specimen

Cross sectional dimensions : (500 x 500) mm			
Series	Top steel (long.)	bottom steel (long)	transverse steel
1	#3 16mm	#11 16mm	10mm @ 100mm c/c

The analytical and experimental results were closely consistent in terms of degree of rotation and stresses in the reinforcements. However the cracking torque predicted by the CA-STM model was higher than the experimental observations. Also the stiffness predicted by the model was lower than the experimental observation.

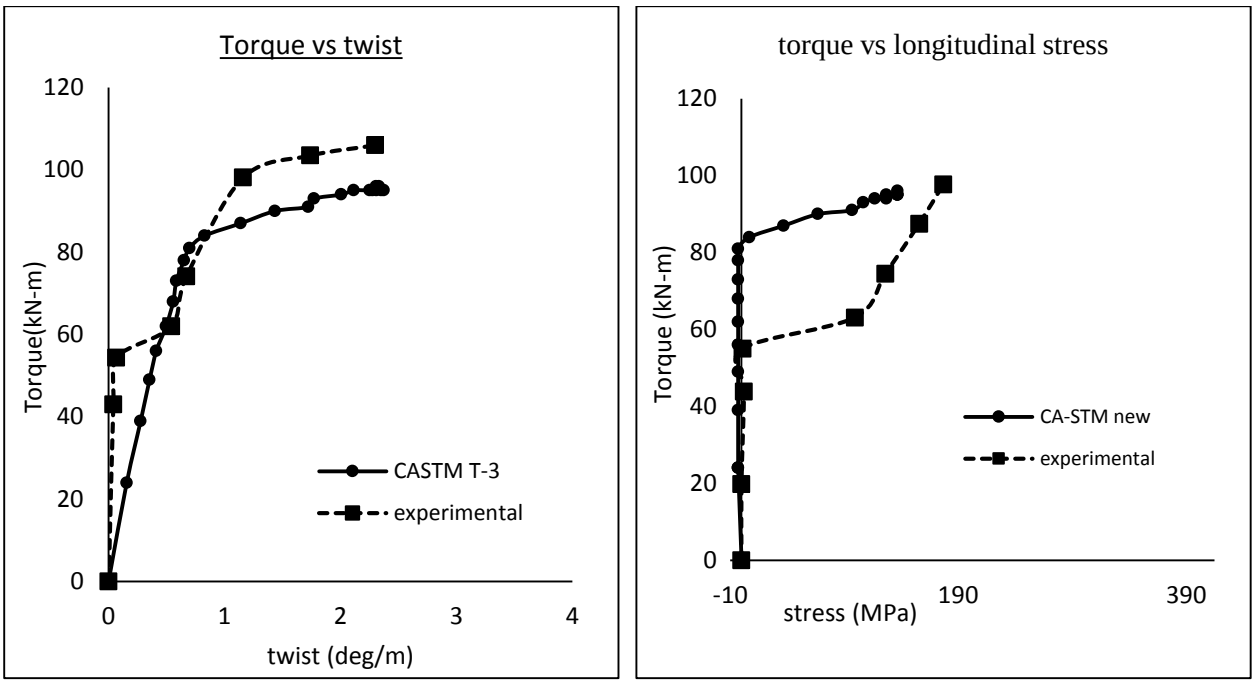

Figure 4.4 Validation of CASTM Model for Pure Torsion

4.3. TORSION COMBINED WITH SHEAR (RAHAL AND COLLINS)

The experimental study was conducted on seven RC beam specimens. The specimens were divided into two series based on the difference in concrete cover. Series 1 and 2 had 3 and 4 numbers of specimens respectively with varying ratios of torque to shear. The specimens used were 6m long with two 3m long transverse wing beams. The difference in forces acting on the wing beams resulted in a torsion in the test region. The schematic representation of the experimental setup is shown in Fig 4.5.

Table 4.3: Specimen details of series 1 and series 2

Series 1	*Series 2*
Dimensions : 600mm x 300mm	Dimensions : 640mm x 340 mm
Transverse reinforcement : 11mm ϕ @ 125mm c/c	Transverse reinforcement : 11mm ϕ @ 125mm c/c
No. of specimens : 3	No. of specimens : 4

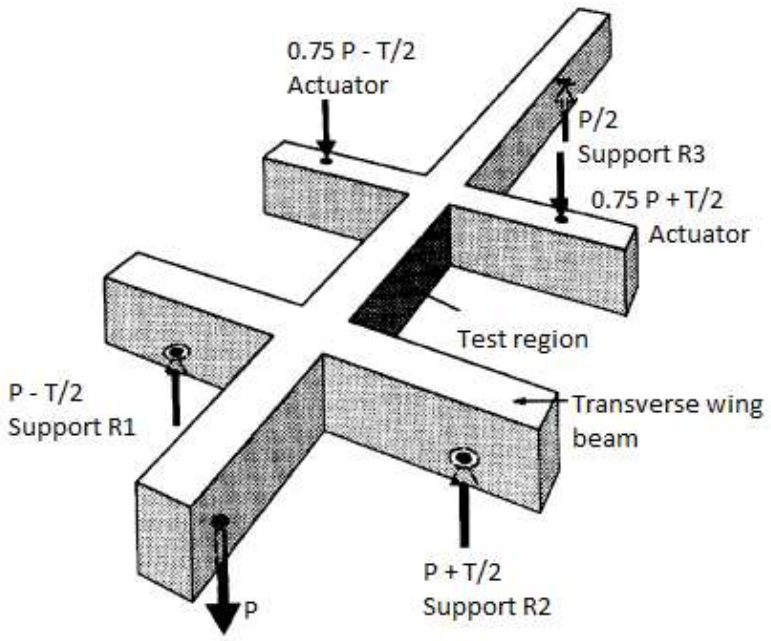

Figure 4.5: Experimental setup of the specimen [Ref. 4]

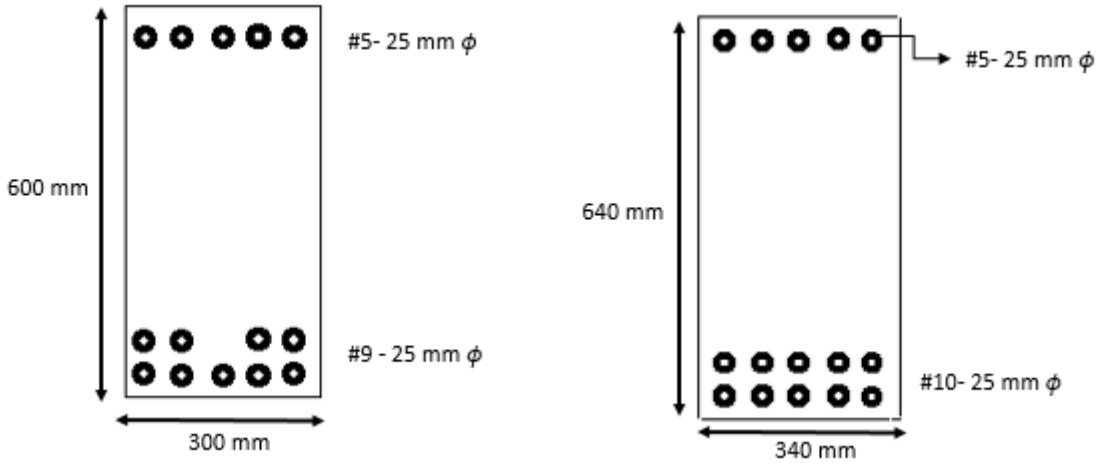

(a) Series 1 (b) Series 2

Figure 4.6: Cross sectional details of the specimens

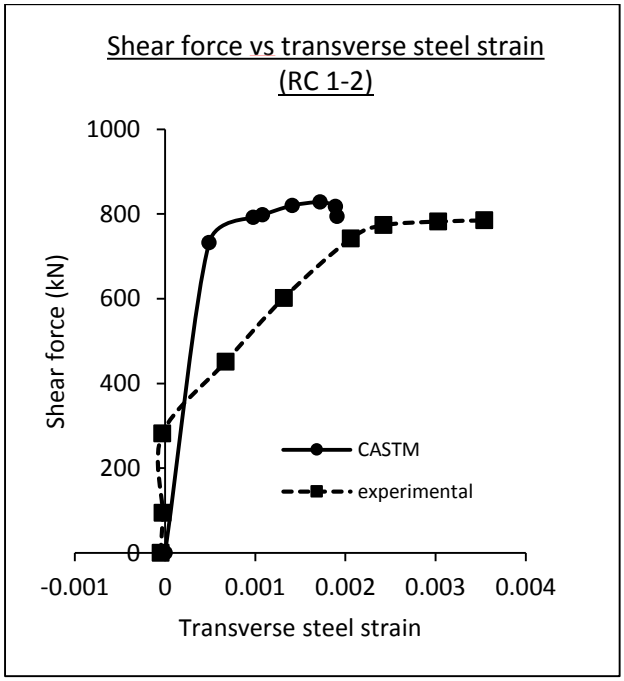

(a) Torque/Shear = 0

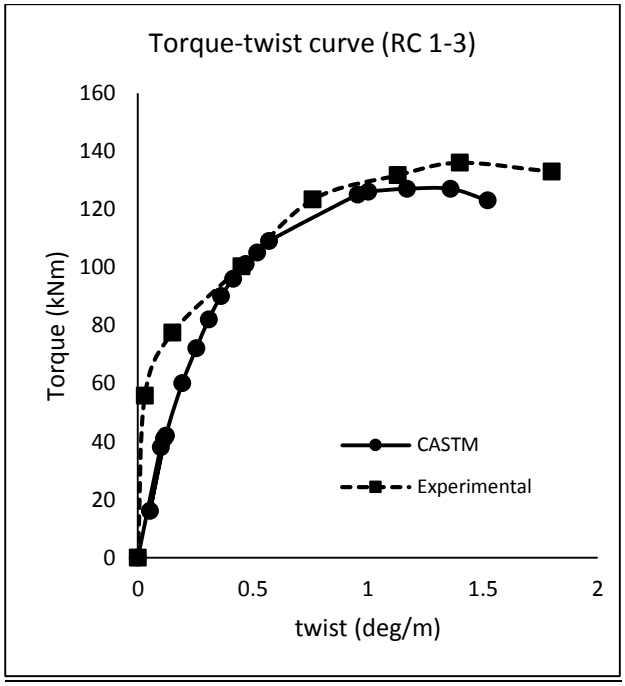

(b) Torque/Shear = 1.3

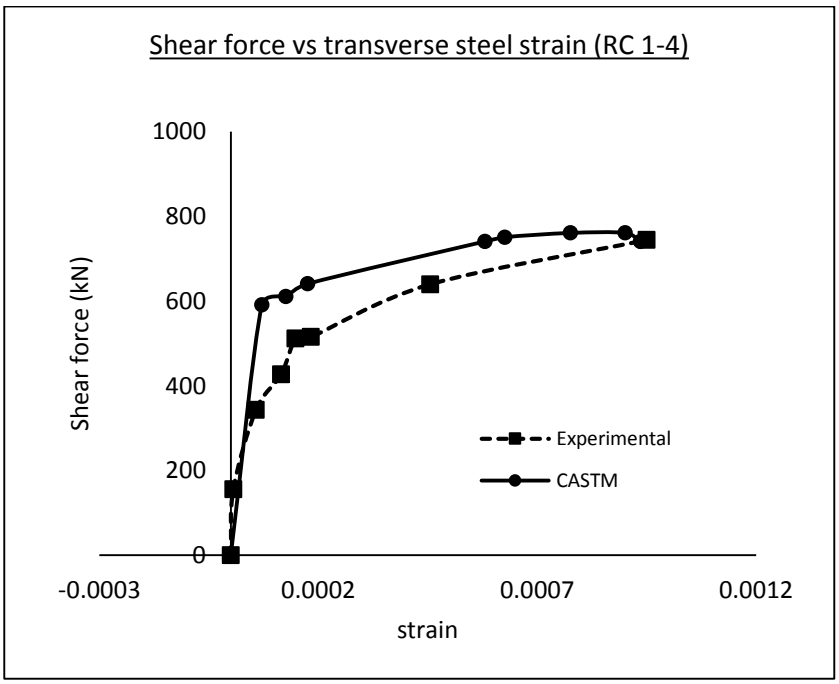

(c) Torque/Shear = 0.01

Figure 4.7: Comparison of results for Series 1

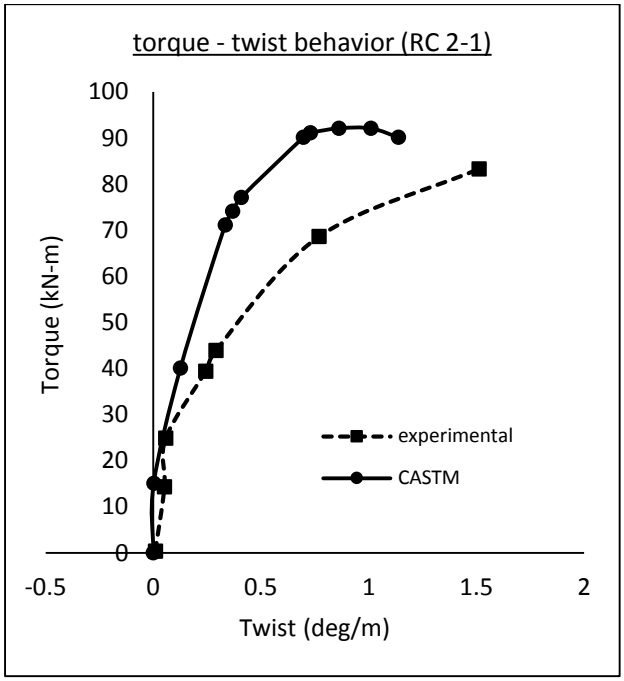

(a) Torque/shear = 0.16

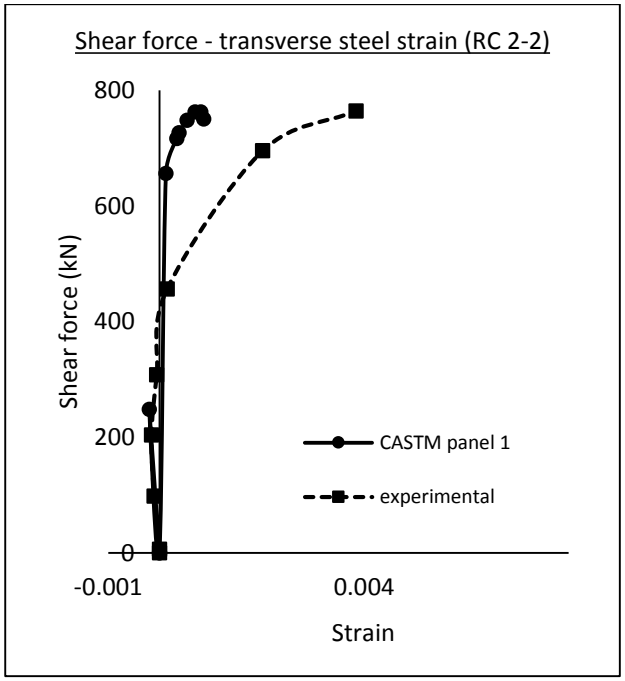

(b) Torque/Shear = 0

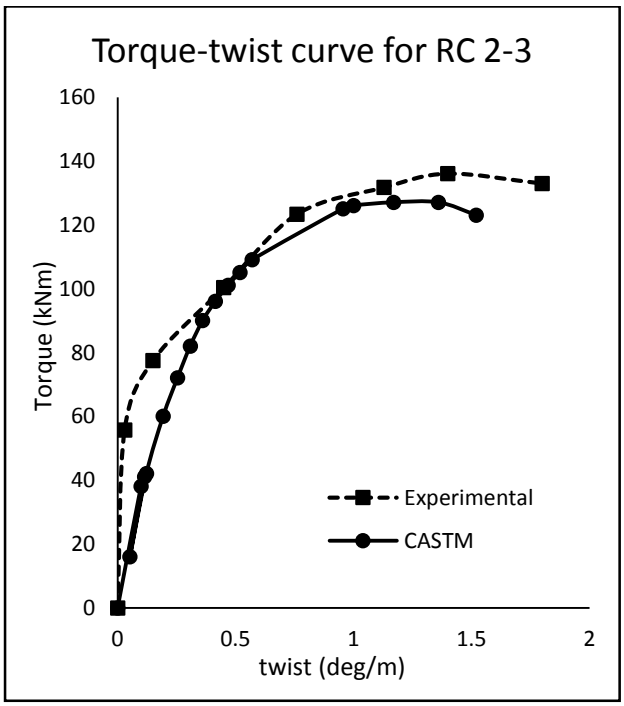

(c)Torque/ Shear = 1.3

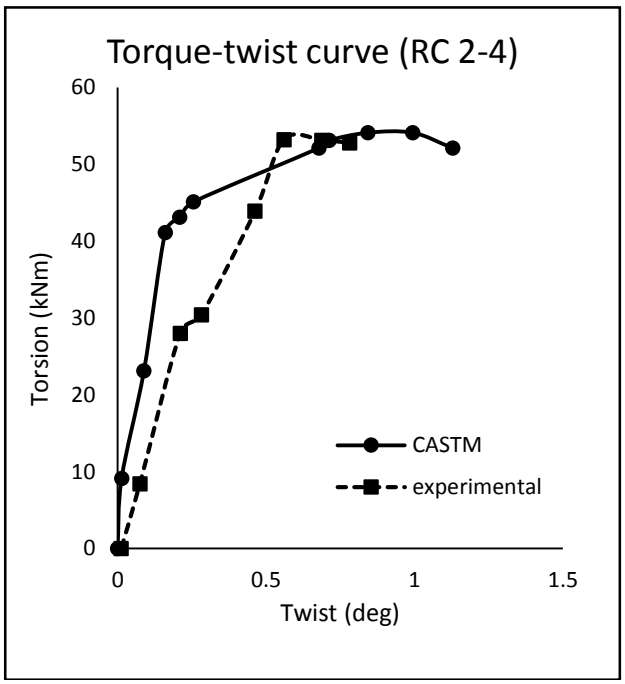

(d) Torque/Shear = 0.08

Figure 4.8: Comparison of results for series 2

The results obtained from CA-STM was in good agreement with the experimental results. The proposed model predicted higher stiffness than the experimental results. The peak values of torsion and shear forces obtained showed a variation of less than 10% from the experimental observations. The values of deformations were accurate with the experimental data.

4.4. TORSION COMBINED WITH AXIAL FORCE AND BENDING MOMENT

The specimens used for the validation of a member subjected to the combination of the forces above were the RC columns tested by Tirasit (2006). The columns were tested for various combinations torque, shear and bending moment. The height of the column was 1.75m. The reinforcement ratio was 1.27%. A constant 160 kN was applied to maintain a normal stress of 1 MPa on the cross section.

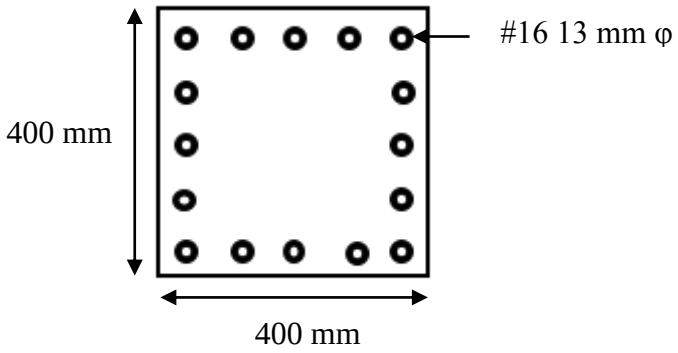

Figure 4.9 Cross section of Tirasit column

Table 4.4 Details of the RC columns (TP-96, TP-98 and TP-99)

Cross sectional dimensions	:	B = 400 mm, H = 400 mm
Concrete compressive strength		31.5 MPa
Yield strength of longitudinal reinforcement		354 MPa

The analytical results matched closely with the experimental results. The peak torque was predicted accurately. However the stiffness of the member before cracking was

under predicted by the model. The peak torque and degree of rotation was predicted accurately with a variation of less than 3%. Thus the model is very efficient in predicting the behaviour of members subjected to bending, torsion and shear to a high degree of accuracy.

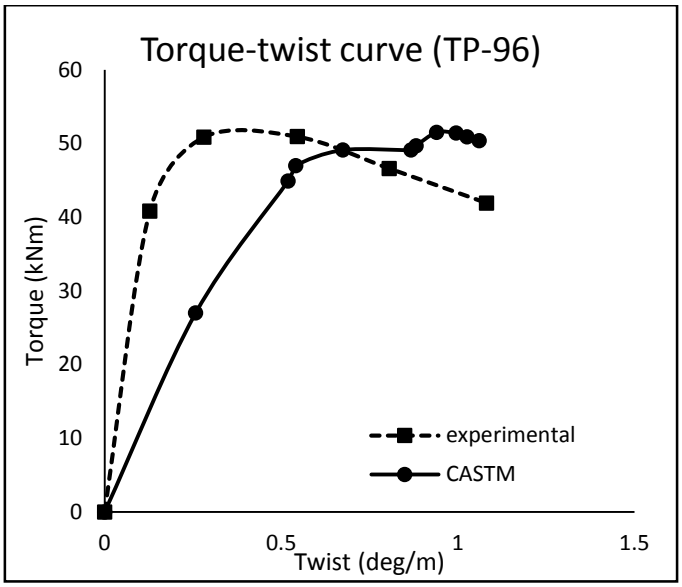

(a) T/M = 0.38, T/V= 0.49

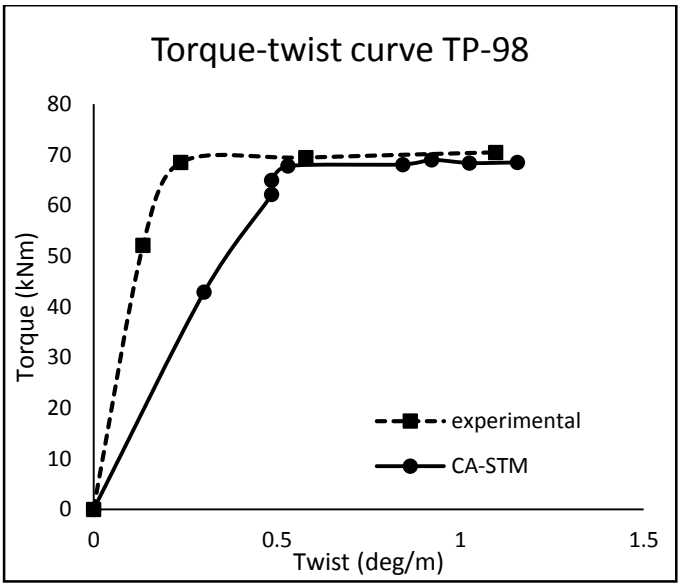

(b) T/M = 0.80, T/V = 0.86

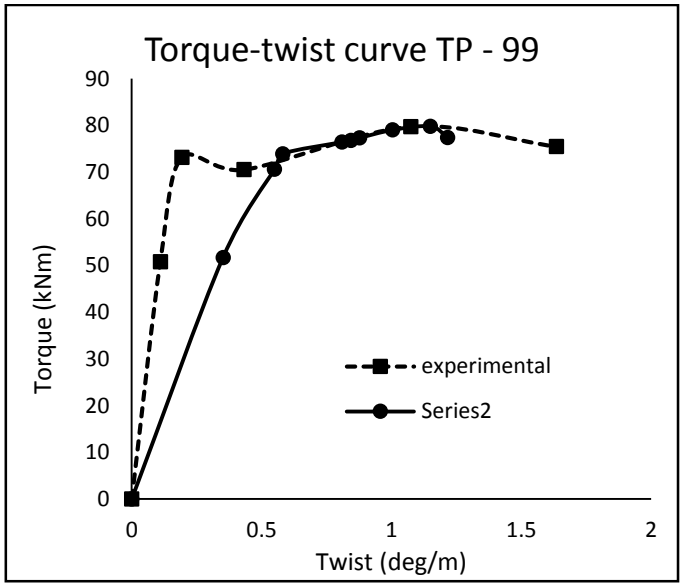

(c) T/M = 1.25, T/V = 1.47

Figure 4.10: Behavior of RC column under combined torsion and bending

Table 4.5 Comparison of results obtained with experimental data

Specimen nomenclature	*Peak Torque*			*Twist*		
	T_{exp}	T_{calc}	T_{exp}/T_{calc}	Θ_{exp}	Θ_{calc}	$\Theta_{exp}/\Theta_{calc}$
McMullen and Warwaruk Specimens (T)						
Series 1	13.2	15.4	0.86	2.760	3.86	0.715
Series 2	18.2	19.9	0.91	3.310	3.55	0.933
Lampert and Thurliamnn Specimens (T)						
T-3	106	96	1.10	2.300	2.33	0.987
Rahal and Collins Specimens (T + V)						
RC 1-2 (T/V = 0)	0	0	1.00	0.0035	0.0017	2.03
RC 1-3 (T/V = 1.31)	136.8	122.1	1.12	3.000	1.63	1.84
RC 1-4 (T/V = 0.01)	0	0	1.00	0.0009	0.0009	1.044
RC 2-1 (T/V = 0.16)	83.3	92.1	0.90	1.512	1.011	1.495
RC 2-2 (T/V = 0)	0	0	1.00	0.0038	0.0008	0.447
RC 2-3 (T/V = 1.22)	136.1	127.1	1.07	1.400	1.36	1.029
RC 2-4 (T/V = 0.08)	53.2	54.1	0.98	0.688	0.994	0.692
Tirasit Specimens (T + V + M)						
TP-096 (T/M = 0.38, T/V= 0.49)	50.928	51.5	0.989	0.545	0.941	0.579
TP-098(T/M = 0.80, T/V = 0.86)	70.478	69	1.021	1.097	0.922	1.189
TP-099(T/M = 1.25, T/V = 1.47)	79.707	79.8	0.998	1.074	1.14	0.942
Average	0.92			1.071		
COV	11.99%			20.6%		

CHAPTER-5

SUMMARY AND CONCLUSIONS

CHAPTER 5

SUMMARY AND CONCLUSIONS

5.1. CONCLUSIONS

The Combined Action Softened Truss Model was studied and it was implemented in Matlab using the latest available constitutive behaviour. The accuracy of the model was validated with test data for three major load combinations.

(a) Pure Torsion: The model could predict the behavior of members under pure torsion reasonably well. The values of peak torque were predicted to an accuracy of 96%. The predictions for twist was relatively less accurate upto 88%. The lower predictions of twist could be due to the limitations in strain relationships used for the formulations.

(b) Torsion combined with Shear: The peak torque prediction was highly accurate for the case of torsion combined with shear. The values varied by less than 3% on an average values from the experimental data. However, the degree of twists predicted were very low in comparison to the experiments. The variations in some cases were as high as 40%.

(c) Torsion combined with shear and bending: The model worked accurately for the prediction of peak torque in this case with an error of less than 1%. The degree of rotation was also predicted reasonably with an error of less than 10%.

5.2. SCOPE FOR FURTHER WORK:

The developed model can be further improved by considering bi-axial effect using the formulations of softened membrane model. Moreover, the effect of cyclic loading also can be included.

5.3 REFERENCES:

Abaqus Analysis User's Manual 6.11. Dassault Systèmes Simulia Corporation, Providence, RI, USA.

Ameli, M, Ronagh, H.R, Dux, P.F (2007). "Behavior of FRP strengthened Reinforced Concrete Beams under Torsion." *Journal of Bridge Engineering*, ASCE library,DOI-10.1061/ASCE-1090-0268-2007

Anand, G. G., Mondal, T. G., Prakash, S. S. (2015). "Improved Softened Membrane Model for Reinforced Concrete Circular Bridge Columns under Torsional Loading". *Journal of Bridge Engineerig*, ASCE library, DOI: 10.1061/(ASCE)BE.1943-5592.0000907.

Belarbi, A., and Hsu, T. T. (1994). "Constitutive laws of concrete in tension and reinforcing bars stiffened by concrete." ACI structural Journal, 91 (4) 465-474.

Chalioris, C. E. (2007). "Analytical model for the torsional behaviour of reinforced concrete beams retrofitted with FRP materials". *Engineering Structures*, 29(12), 3263-3276.

Claeson, C. and Johansson, M. (1999). "Finite element analysis of confined concrete columns." *Proceedings of the fifth international symposium on utilization of high-strength/high-performance concrete*, Sandefjord, Norway.

Delso, J. M., Stavridis, A., and Shing, B. (2011). "Modeling the Bond-Slip Behavior of Confined Large Diameter Reinforcing Bars." *III ECCOMAS Thematic Conference on Computational Methods in Structural Dynamics and Earthquake Engineering COMPDYN*, Corfu, Greece.

Floros, D., and Ingason, O. A. (2013). "Modeling and Simulation of Reinforced Concrete Beams: Coupled Analysis of Imperfectly Bonded Reinforcement in Fracturing Concrete." Master's Thesis 2013:42, Department of Applied Mechanics: Division of Solid Mechaics, Goteborg, Sweden.

Hadi, M.N.S (2006). "Behavior of FRP wrapped normal strength concrete columns under eccentric loading." *Engineering Structures Journal*, Elesvier,72,pp 503-511.

Hsu, T. T. C. (1968a). "Torsion of Structural Concrete - Behavior of Reinforced Concrete Rectangular Members." *Torsion of Structural Concrete, SP-18, American Concrete Institute*, Detroit, MI.

Hurtado, G. (2009). "Effect of Torsion on the Flexural Ductility of Reinforced Concrete Bridge Columns." Ph.D. Thesis, Department of Civil and Environmental Engineering, University of California, Berkeley.

Jankowiak, T., and Lodygowski T. (2005). "Identification of Parameters of Concrete Damage Plasticity Constitutive Model." *Foundations of Civil and Environmental Engineering*, No. 6.

Jeng, C. H., and Hsu, T. T. (2009). "A softened membrane model for torsion in reinforced concrete members." *Engineering Structures,* 31(9), 1944-1954.

Mitchell, D. and Collins, M. P. (1974). "Diagonal Compression Field Theory - A Rational Model for Structural Concrete in Pure Torsion." *Journal of the American Concrete Institute, 71,* pp. 396-408.

Mondal, T. G., and Prakash, S. S. (2015). "Nonlinear Finite-Element Analysis of RC Bridge Columns under Torsion with and without Axial Compression." *Journal of Bridge Engineering, ASCE library,* 04015037.

Mondal, T. G., & Prakash, S. S. (2015). "Effect of tension stiffening on the behavior of reinforced concrete circular columns under torsion". *Engineering Structures,* 92, 186-195.

Panchacharam, S and Belarbi, A "Torsional Behavior of Reinforced Concrete Beams Strengthened with FRP Composites," First FIB Congress, Osaka, Japan, October-2002

Prakash, S. S. (2009). "Seismic Behavior of RC Circular Columns under Combined Loading Including Torsion." Department of Civil Engineering, Missouri University of Science and Technology, Missouri, USA.

Rabbat, B. G., and Russell, H. G. (1985). "Friction Coefficient of Steel on Concrete or Grout." *Journal of Structural Engineering,* ASCE 111(3): 505-515.

Rahal, K. N., and Collins, M. P. (1996). "Simple Model for Predicting Torsional Strength of Reinforced and Prestressed Concrete Sections." *ACI Structural Journal*, 93, 658-666.

Rutledge, S.T., Kowalsky, M.J., Seracino, R., Nau, J.M. (2012). "Repair of Damaged Circular Reinforced Concrete Columns by Plastic Hinge Relocation." 15WCEE, LISBOA 2012, North Carolina State University, USA.

Suman Dhara (2015)." Behavior of Precast Prestressed Hollow Core Slabs with and without FRP Strengthening." Department of Civil Engineering, Indian Institute of Technology, Hyderabad, India.

Tirasit, P., and Kawashima, K. (2007a). "Seismic performance of square reinforced concrete columns under combined cyclic flexural and torsional loadings." *Journal of Earthquake Engineering,* 11, 425-452.

Tirasit, P., and Kawashima, K. (2007b). "Effect of nonlinear torsion on the performance of skewed bridge piers." *Journal of Earthquake Engineering,* 12, 980-998.

Vecchio, F. J., and Collins, M. P. (1986). "The Modified Compression-Field Theory for Reinforced Concrete Elements Subjected to Shear." *Journal of the American Concrete Institute,* 83, 219-231.

Wang, J. (2006). "Constitutive relationships of prestressed concrete membrane elements." Ph.D. thesis, Dept. of Civil and Environmental Engineering, Univ. of Houston, Houston.

Zhang, L. X. (1995). “Constitutive laws of reinforced elements with high strength concrete.” Ph.D. thesis, Dept. of Civil and Environmental Engineering, Univ. of Houston, Houston.

Zhu, R. R., and Hsu, T. T. (2002). “Poisson effect in reinforced concrete membrane elements.” *ACI Structural Journal*, 99 (5), 631-640.